
Synthetic Diamonds as Pulse Counting Radiation Detectors

Paul Joseph Fallon

Degree awarded with distinction 13 December 1989

Submitted for the degree of Master of Science
University of the Witwatersrand, Johannesburg
August 1989

Abstract

Synthetic diamonds were adapted for use as pulse-counting radiation detectors. When used as dosimeters to measure γ -rays, dose rates as low as $1 \mu\text{Gy}\cdot\text{h}^{-1}$ were recorded, the response was linear over six orders of magnitude and was shown to be energy independent.

Opposite parallel faces of the diamonds were prepared as contacts by ion implantation techniques. The contacts suppressed the development of space charge, resulting in consistent count rates being recorded.

For best response the diamonds were first primed with a large γ -ray dose. Exposure of the diamonds to ambient light returned them to the unprimed state. This effect has been used to measure the energy of the trapping level that is populated by pre-irradiation and depopulated by exposure to light.

The pulse counting and scintillation responses were found to increase with decreasing single substitutional nitrogen concentration, indicating that the single substitutional nitrogen centre behaves as a charge carrier recombination centre.

No γ -ray or α -particle energy resolution was possible using these pulse counting diamond detectors. It is believed that this was due to the presence of charge carrier trapping and recombination centres within the diamonds.

I declare that this dissertation is my own, unaided work. It is being submitted for the degree of Master of Science in the University of the Witwatersrand, Johannesburg. It has not been submitted before for any degree or examination in any other university.

Paul Fallon

8th day of August, 1989 .

To my parents

Acknowledgements

I would like to thank everyone who has been involved with the project during the last eighteen months, it has proven an enjoyable and outstanding educational experience.

- o Professor R. J. Keddy, my supervisor, who made this fascinating project available. I am grateful to him for always being available, for his willingness to discuss the project and for offering helpful advice and guidance.
- o Tom Nam for his assistance and friendship. His knowledge about the subject, willingness to discuss and follow the progress of the project were constant sources of inspiration and encouragement.
- o The De Beers Diamond Research Laboratory for their enthusiastic and encouraging support, in particular Dr. Rob Caveney, Dr. Robbie Burns who produced the synthetic diamonds and Kobus Grobbelaar who designed and built the pulse counting electronics and taught me the subtleties of its workings.
- o Professor J. P. F. Sellschop for his constant support and encouragement of the project, and for the loan of a suite of natural type IIa diamonds.
- o Dr. Johan Prins who gave me excellent advice on making electrical contacts to diamonds.
- o The staff and students of the Schonland Research Centre, in particular :
 - Mick Rebak for his excellent technical assistance and for allowing me the use of facilities in his laboratory.
 - Hugo Andeweg for his help with conventional electronics.
 - Ian McKowen and Ian McQueen for their professionally made diamond holders.
 - John Beer for his constant willingness to help.

- Rosemary Cawood for operating the ion implanter during many of the implantations.
 - Professor Harold Annegarn, Dr. Trevor Derry and Dr. Roger Fearick for their willing and wholehearted help and advice.
 - My fellow students Raymond Spits, Elias Sideras-Haddad, Sanjiv Shrivastava, Alfred Hoernle for their help and friendship on a day-to-day basis.
- o I am also grateful to the members of the Physics Department for their help, in particular Dr. J. A. van Wyk who made his laboratory available and taught me about ESR measurements of diamond, and Professor J. D. Comins who loaned me a monochromator and for trusting me to operate his Cary Spectrophotometer.
- o Last and not least I would like to thank Mrs. Rosamund Naoumoff for the loan of a personal computer on which most of this thesis was compiled, and my father, Martin Fallon, for painstakingly checking the grammar.

CONTENTS

Chapter 1. Introduction	1
1.1 Introductory description	1
1.2 Literature survey	2
1.3 Motivation	4
Chapter 2. Theory	6
2.1 Interactions of γ -rays with matter	6
2.2 Diamond structure and types	9
2.3 Band structure	10
2.4 The Hecht Function	12
Chapter 3. Experiment	14
3.1 Preparation of diamonds	14
3.2 Electronic circuitry	16
3.3 Radiation sources	22
Chapter 4. Pulse-counting results	23
4.1 Introduction	23
4.2 Different electrical contacts tested	27
4.3 The boron <i>p</i> -doped contact	29
4.4 Pre-irradiation	30
4.5 The effect of using different radiation sources	34
4.6 Alpha particle measurements	35
4.7 Dose rate measurements	36

Chapter 5. The effect of light	41
5.1 Introduction	41
5.2 Photoconduction	43
5.3 Wavelength causing depopulation	45
5.4 Shallow trapping levels	48
5.5 The pre-irradiation trapping level	50
5.6 Conclusion	53
Chapter 6. Scintillation counting	54
6.1 Introduction	54
6.2 Method	54
6.3 Results	56
6.4 Conclusion	61
Chapter 7. Nitrogen	62
7.1 Introduction	62
7.2 ESR techniques and measurements	63
7.3 Results	67
7.4 Discussion	71
Chapter 8. Discussion of Results	72
8.1 Number of pulses recorded	72
8.2 The space charge	73
8.3 Effect of potential across diamond (Hecht function)	76
8.4 The shape of the pulse height spectrum	78
8.5 Energy dependance of the pulse height distribution	81
Chapter 9. Conclusion	83
9.1 Summary of results	83
9.2 Ideas for further research	84

Appendix A : List and description of diamonds	87
Appendix B : Circuit diagrams	98
Appendix C : Papers, Patents and Conferences	101
References	102

List of Figures

Figure 2.1	6
	Electromagnetic radiation total mass attenuation coefficient for Carbon.	
Figure 2.2	8
	Pulse height spectrum obtained from a ^{137}Cs γ -ray source.	
Figure 2.3	10
	Unit cubic cell of diamond lattice.	
Figure 2.4	11
	Band structure of diamond.	
Figure 3.1	17
	Schematic diagram of circuit used for pulse counting measurements.	
Figure 3.2	19
	A typical ^{137}Cs γ -ray spectrum, using a synthetic diamond detector and custom built electronics.	
Figure 3.3	19
	A typical ^{137}Cs γ -ray spectrum, using a synthetic diamond detector and conventional electronics.	
Figure 3.4	20
	Circuit diagrams for connections between diamond, high voltage power supply and load resistor.	
Figure 3.5	21
	Plot of count rate versus potential.	
Figure 4.1	24
	Pulse counting rate measured as a function of time.	
Figure 4.2	24
	Initial pulse height spectrum and spectrum recorded three hours later.	

Figure 4.3	25
Count rate of a diamond counter, with polarity of high voltage across diamond switched at two minute intervals.		
Figure 4.4	28
Count rate as a function of time, showing the effect of ion implanting both polished surfaces with carbon.		
Figure 4.5	28
Count rate as a function of dose rate, showing the effect of ion implanting both polished surfaces with carbon.		
Figure 4.6	29
Count rate as a function of time for diamond with boron <i>p</i> -doped and carbon ion implanted contacts.		
Figure 4.7	30
Count rate as a function of time for diamond with two boron <i>p</i> -doped contacts.		
Figure 4.8	31
Count rate for diamond with polarity of high voltage switched at two minute intervals.		
Figure 4.9	32
Diamond with a boron <i>p</i> -doped contact, not exposed to light.		
Figure 4.10	32
Pulse height spectra showing the effect of pre-irradiation and the effect of exposing a pre-irradiated diamond to light.		
Figure 4.11	33
Count rate for pre-irradiated diamond with a boron <i>p</i> -doped and a carbon ion implanted contact, measured once or twice a day for seven days.		
Figure 4.12	33
Pulse counting measurements performed after pre-irradiation and after two eleven day periods.		
Figure 4.13	34
Pulse height spectra of various radiation sources, using pulse counting diamond detector.		
Figure 4.14	35
Pulse height spectrum of ²⁴¹ Am α -particles incident on polished face between contacts.		

Figure 4.15	Count rate as a function of the dose rate of ^{137}Cs γ -rays.	38
Figure 4.16	Count rate for irradiation from different sources.	38
Figure 4.17	Dose rate response for irradiation from different sources.	39
Figure 4.18	Dose rate response for diamond with carbon fibre contacts attached by means of carbon epoxy dag.	39
Figure 5.1	Diamond counting overnight in the dark.	41
Figure 5.2	Thermoluminescent spectra of diamond suite 2 no. 2.	42
Figure 5.3	Intensity of the monochromator light as a function of wavelength.	44
Figure 5.4	A typical photoconduction spectrum.	44
Figure 5.5	Schematic diagram of the photoconduction circuit.	45
Figure 5.6	Effect on the pulse counting response as a function of wavelength after exposing the diamond to light.	47
Figure 5.7	Effect on the pulse counting response as a function of energy after exposing the diamond to light.	47
Figure 5.8	Procedures affecting the shallow hole traps in diamond.	49
Figure 5.9	Band structure diagram with the trapping level which causes decreased counting response.	51

Figure 6.1	55
Schematic diagram of apparatus to measure scintillation spectra of diamond.	
Figure 6.2	58
Typical scintillation spectrum from synthetic diamond used for pulse counting measurements.	
Figure 6.3	58
Scintillation spectrum of an iron free synthetic diamond.	
Figure 6.4	59
Scintillation spectra for two surfaces of the same synthetic diamond.	
Figure 6.5	59
Scintillation spectra for two different intensities of 5.5 MeV α -particle sources, both incident on the same position of a synthetic diamond.	
Figure 6.6	60
Phosphorescence decay curves from Nam et al 1989.	
Figure 7.1	63
Schematic diagram of the single substitutional nitrogen impurity in the diamond lattice.	
Figure 7.2	64
Electron energy level splitting for the single substitutional nitrogen impurity in diamond.	
Figure 7.3	65
ESR spectra of single substitutional nitrogen in diamond at 22 °C.	
Figure 7.4	66
A typical ESR spectrum.	
Figure 7.5	66
The ESR spectrum in figure 7.4 integrated twice.	
Figure 7.6	70
Pulse counting response as a function of single substitutional nitrogen concentration.	
Figure 7.7	70
Scintillation counting response as a function of single substitutional nitrogen concentration.	

Figure 8.1	Percentage of incident γ -rays that will interact with a diamond 1 mm thick.	72
Figure 8.2	Count rate as a function of the time after pre-irradiation.	73
Figure 8.3	Count rate for diamond CoFe stone 6 with boron-doped and carbon ion implanted contacts.	75
Figure 8.4	Hecht function fit for the pulse counting rate as a function of potential across the diamond contacts.	77
Figure 8.5	Pulse height spectra for the SIN 12 diamond.	80
Figure 8.6	Inverse of the semi-log slope of the pulse height spectrum as a function of radiation energy.	81
Figure A.1	Thermoluminescent spectrum of CoFe stone 10.	94
Figure A.2	Thermoluminescent spectrum of 691 stone 9 and 10.	95
Figure A.3	Thermoluminescent spectrum of Suite 2 no. 3.	95
Figure A.4	Thermoluminescent spectrum of Suite 1.	96
Figure A.5	Thermoluminescent spectrum of SIN 12.	96
Figure A.6	Thermoluminescent spectrum of SIN 11.	97
Figure A.7	Thermoluminescent spectrum of SIN 3.	97

Figure B.1	98
Schematic diagram of custom built pulse counting circuit.		
Figure B.2	99
Circuit diagram of custom built differential pulse amplifier.		
Figure B.3	100
Custom built test circuit for diamond pulse and conduction counter.		

List of Tables

Table 7.1	67
Average single substitutional nitrogen concentration for types of synthetic diamonds, their saturation pulse counting response and their scintillation counting response.	

Chapter 1. INTRODUCTION

1.1 Introductory description

In this investigation synthetic and natural diamonds have been adapted for the detection of γ -rays by monitoring the electric pulses generated by radiation interacting with the diamond. This method of radiation detection is similar to that employed by a silicon surface barrier detector. Electrical contacts are made to two opposite parallel polished faces of the diamond and a high voltage is applied across the contacts. Radiation interacting with the diamond excites electrons from the valence band to the conduction band. The excited electrons and the holes remaining in the valence band move under influence of the electric field created by the high voltage across the diamond contacts and appear as electrical pulses in the high voltage circuit. The electric pulses are amplified by a pre-amplifier, positioned close to the diamond, and by a main amplifier, and are then recorded. The number and sizes of the pulses are used as a measure of the incident radiation, as the size of the pulse should be proportional to the energy deposited by the incident radiation, and the number of pulses is the number of radiation interactions with the diamond.

The use of diamonds as radiation detectors is investigated, even though other detectors are available, since diamond detectors will have unique applications in the medical and health physics fields. The electron density of diamond (atomic number 6) is similar to that of human tissue (average atomic number of 7.4), and thus diamond and human tissue will exhibit similar radiation absorption characteristics. The diamond will not be seen as an artifact by the radiation field. It is usually only a few cubic millimeters in size, is non-toxic and chemically stable, making it ideal for in vivo measurements. The small size will also allow 'pin point' measurements to be performed, instead of average values obtained from larger volume detectors.

Many studies have been made into the use of natural diamonds as pulse-counting radiation detectors, but only limited success has been reported (cf. section 1.2). The main problems were, and still are, understanding the type of diamonds that make good counters and the reasons for good or poor counting performance. Only a few natural diamonds show good counting properties and the process of selecting a 'good stone' requires the testing of many diamonds before a suitable specimen is found.

Improved synthesizing techniques have created a new optimism about the possibility of commercially producing diamond detectors, and the ability to reproduce the correct type of stone will eliminate the need for lengthy selection processes. With present synthesizing techniques the chemistry of the process can be controlled so as to influence properties of the diamond by increasing or decreasing impurity concentrations.

The aim of this investigation was the development of a pulse counting diamond radiation detector, leading towards the commercial production of such devices. The investigation has centered around understanding the physical properties of diamond which influence the radiation detection and using this understanding to solve problems in developing a pulse counting diamond radiation detector. The problems do not originate from the manner in which radiation interacts with diamond, as these processes are understood, but occur from the transport of charge carriers released by radiation interactions and are thus fundamentally solid state problems. The problems have been solved to the extent that an effective pulse counting diamond detector has been produced, even though limited in its applications. It is reported in this thesis that radiation detection using the diamond in a pulse counting mode can and has been used as a tool to investigate trapping and recombination centres in diamond.

1.2 Literature survey

Diamond was the first material to be used in an attempt to develop a pulse counting crystal radiation detector, since it had properties most suitable for pulse counting detection (van Heerden 1945). The experiments were unsuccessful, and van Heerden went on to show that silver chloride could count β -particles, thus making silver chloride the first pulse counting crystal radiation detector. The disadvantage of silver chloride was that it was only able to count when cooled to the temperature of liquid air. Two years later Wooldridge et al (1947) detected α -particles using diamonds in a pulse

counting mode, and two weeks after their discovery Curtiss and Brown (1947) detected γ -rays with a pulse counting diamond detector. These discoveries with diamond were the first detections of radiation using a pulse counting crystal detector at room temperature.

Many subsequent reports describing pulse counting diamond radiation detectors followed: Wouters and Christian (1947), Chynoweth (1947), McKay (1948), Hofstadter (1948, 1949a,b), Willardson and Danielson (1950), Willardson (1950), Cotty (1956a,b), Champion and Dale (1956), Champion and Wright (1959), Kennedy (1959), Urlau (1960), Urlau et al (1960), Afanas'eva and Konorova (1964), Champion and Kennedy (1965), Vermeulen (1965) and Vermeulen and Nabarro (1967b). In all the above investigations problems were encountered with the selection of pulse counting diamonds and polarization of the diamonds during pulse counting. Very few of the diamonds that were tested made good radiation counters and no method of selecting pulse counting diamonds, other than testing the pulse counting response, was known. Curtiss and Brown (1947) report that only two diamonds out of one hundred tested were able to detect γ -rays. Polarization (the space charge effect) occurred in the diamonds that were tested and took place because a space charge field developed within the diamond opposing the externally applied electric field. As the space charge developed, the pulse size was reduced and the counting rate decreased (Cotty 1956b). Methods of reducing the space charge effect were discovered - switching the polarity of the applied electric field (Wouters and Christian 1947, McKay 1948, Hofstadter 1949a), and exposing the diamond to red light (Chynoweth 1947, Willardson and Danielson 1950, Urlau et al 1960, Vermeulen and Nabarro 1967b). The problems of selection and the inability to alter the impurity and defect concentration, or to identify many of the defects and impurities in diamond, made it impossible to identify and remove the cause of the space charge. This and the unavailability of a large supply of pulse counting diamonds caused a reduction in the investigations of pulse counting diamonds in favour of other more available and workable materials (e.g. silicon).

It was only in 1971 that the first space charge free pulse counting diamond detector was reported (Konorova and Kozlov 1971). They claim to have removed the space charge effect by creating a 'hole injection' contact, and claim to detect α -particles with a good energy resolution. Other investigations have followed in which the 'hole injection' contact has been used to create space charge free pulse counting diamond detectors. (Kozlov and Konorova 1972, Kozlov et al 1975, Kozlov et al 1977, Canali et al 1979,

Nava et al 1979, de Blasi et al 1979). The above reports on the 'hole injection' pulse counting diamond detectors have described the physical properties of the diamond, but no mention of the practical uses of such devices has been reported, although possible uses have been described.

So far no energy resolution for γ -ray or X-ray detection using a pulse counting diamond detector has been reported. Until the investigation described in this thesis, no reports have appeared on the investigation, use or development of *synthetic* pulse counting diamond detectors.

Other methods of detecting radiation using diamond as the detector are also possible, and have been investigated and reported on in the literature. Charge carriers freed by radiation interactions can be trapped at trapping centres in the diamond, and are released if the diamond is heated. The released charge carriers can recombine at luminescent centres in the diamond, producing light which can be measured. The procedure is termed thermoluminescence, and the amount of light produced when the diamond is heated is used as a measure of the radiation which was incident on the diamond (Nam et al 1987, Eliseev et al 1988, Nam 1989). The electrical conduction of the diamond can be used to measure radiation doses. Ionization by interacting radiation will increase the electrical conductance of the diamond, and can be measured by placing the diamond in a simple d.c. resistance measuring circuit (Kozlov et al 1977, Burgemeister 1982, Keddy et al 1988). The diamond can be used as a scintillation counter - the charge carriers freed by radiation interactions can recombine immediately at luminescent centres, producing light that can be measured using a photomultiplier tube (Ralph 1959, Nam et al 1989). The diamond can be used as a bolometer - if cooled to about 1 K, the thermal spikes caused by interacting radiation can be recorded and used as a measure of the incident radiation, in a similar way to the pulses from a pulse counting detector. Using a diamond bolometer Coron et al (1985) have been able to detect α -particles with reasonable energy resolution.

1.3 Motivation

The unique applications of diamond radiation detectors as dosimeters in the medical and health physics fields has lead to renewed interest in their development. Bampton (1976) has reported on the development of a pulse counting natural diamond radiation

detector and its use in a hospital environment. The development of synthetic diamonds has introduced a method of creating 'tailor-made' and reproducible specimens. This eliminates the lengthy selection processes required to find the correct type of natural diamond for radiation detection purposes and creates a method to investigate the effect of different impurities in diamonds. These developments have motivated the investigation reported in this thesis. The investigation follows from and thermoluminescent and d.c. conduction radiation detection investigations using synthetic diamonds, which were conducted by Professor R. J. Keddy and Mr. T. L. Nam at the Schonland Research Centre, University of the Witwatersrand, Johannesburg.

Chapter 2. THEORY

2.1 Interactions of γ -rays with matter

There are three major processes by which electromagnetic radiation interacts with matter - photoelectric absorption, Compton scattering and pair production. Other minor processes exist but are negligible compared to the three major processes. The number of photons that will interact with a material is governed by the interaction cross section which differs between these processes and depends on the photon energy and the material with which the photon interacts (figure 2.1).

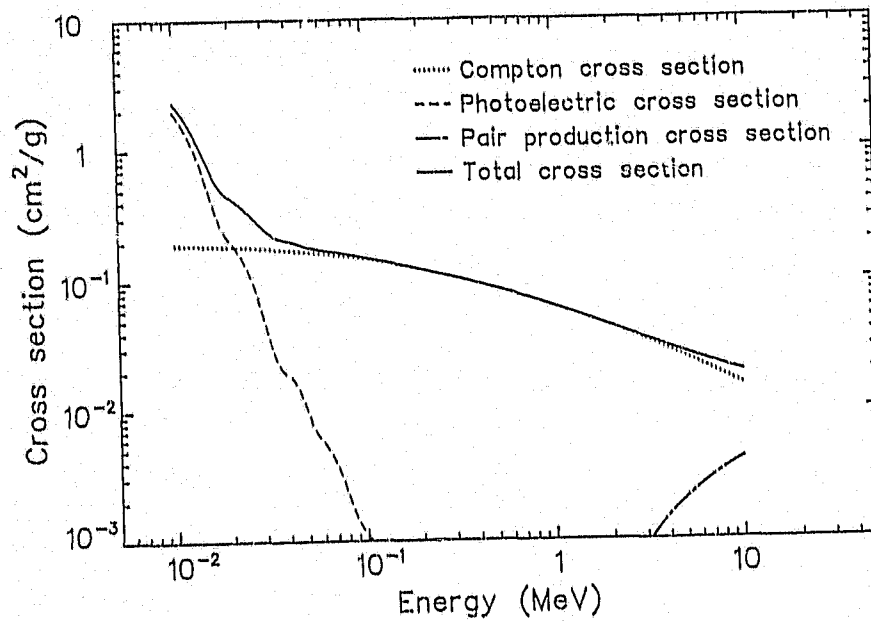


Figure 2.1. Electromagnetic radiation total mass attenuation coefficient (interaction cross section) for Carbon.

Electromagnetic radiation exhibits a characteristic exponential absorption in matter since each photon interacts individually in a single event. The number of photons that will pass through a material of thickness, x , is given by

$$n_r = n_0 e^{-\sigma \rho x} = n_0 e^{-\mu x} \quad (2.1)$$

for n_0 initial photons, total attenuation coefficient σ (plotted in figure 2.1), and density ρ . The number of photons interacting with the material of thickness, x , is thus

$$n_x = n_0(1 - e^{-\mu x}). \quad (2.2)$$

For a majority of the experiments a ^{137}Cs γ -ray radiation source was employed and produced γ -rays of energy 661.2 keV. The major energy absorption process by diamond at this energy is Compton scattering, in which an atomic electron scatters the γ -ray and energy and momentum are transferred to the electron. The highly energetic electron loses most of its energy by interaction with other electrons. These electrons are excited to the conduction band, creating free electrons in the conduction band and free holes in the valence band which are measured and indicate that an interaction took place. A fixed amount of energy is required to excite the electrons to the valence band and thus the number of electrons and holes (charge carriers) produced is proportional to the energy lost by the γ -ray.

The energy absorbed by the electron depends on the angle of scattering and is described by

$$E = E_0 - \frac{E_0}{1 + (E_0/m_e c^2)(1 - \cos \theta)} \quad (2.3)$$

where E_0 is the incident γ -ray energy,

m_e is the electron rest mass,

c is the speed of light, and

θ is the γ -ray scattering angle.

The maximum energy transferred to the electron by Compton scattering, will occur at $\theta = 180^\circ$ and will have a value of

$$E_{max} = E_0 - \frac{E_0}{1 + 2E_0/m_e c^2} \quad (2.4)$$

The differential scattering cross section, describing the energy distribution can be obtained (Segrè 1953) and the number of interactions transferring energy E to the scattering electron is proportional to

$$f(E) = \frac{E_0}{E_0 - E} \left[1 + \left(\frac{E_0 - E^2}{E_0} \right) - \frac{2(\gamma + 1)}{\gamma^2} - \frac{1 + 2\gamma}{\gamma^2} \left(\frac{E_0 - E}{E_0} \right) + \frac{1}{\gamma^2} \left(\frac{E_0}{E_0 - E} \right) \right] \quad (2.5)$$

for energies of zero to E_{max} , where $\gamma = E_0/m_e c^2$. The energy transferred to the electron by Compton scattering produces a rectangular shaped region in the pulse height spectrum up to a maximum energy E_{max} (figure 2.2). Because of detector resolutions, the spectra obtained are the theoretically expected spectra convoluted with a gaussian resolution.

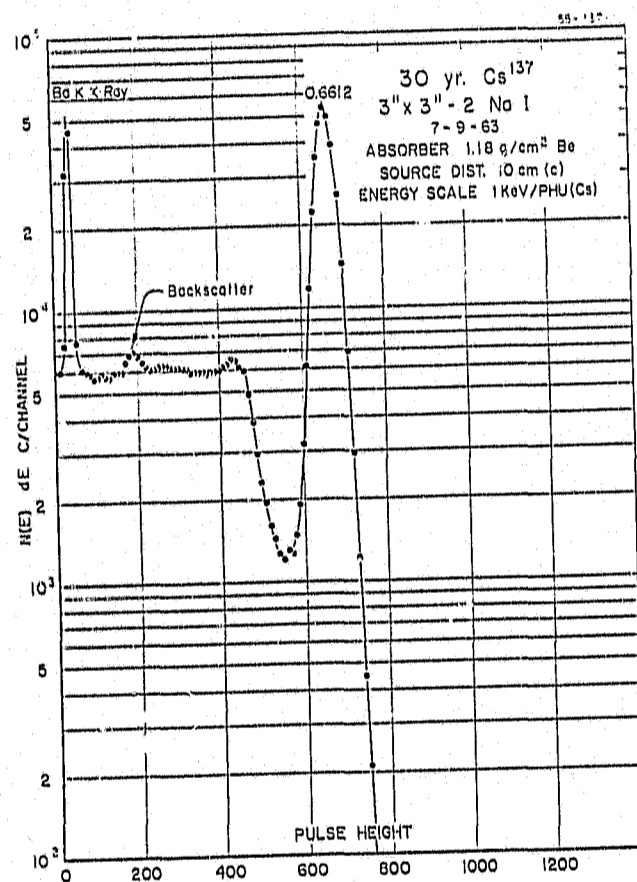


Figure 2.2. Pulse height spectrum obtained from a ^{137}Cs γ -ray source. (Taken from Heath 1964).

A peak corresponding to the 661.2 keV γ -ray energy will appear if single or multiple Compton scattering occurs followed by photoelectric absorption. The probability of all

the 661.2 keV γ -ray energy being absorbed by photoelectric absorption is negligible since the photoelectric cross section for diamond is extremely small at 661.2 keV (cf. figure 2.1). Pair production will not occur at this energy as at least 1.022 MeV is required to produce an electron positron pair. Since the diamonds have a small volume it is unlikely that multiple absorption events will occur within the diamond and therefore it is unlikely that the 661.2 keV γ -ray peak will be observed in the spectrum. It is expected that only a modified rectangular shaped Compton region will appear in the ^{137}Cs spectrum.

2.2 Diamond structure and types

Diamond is valuable as a gem stone because of its high refractive index and its high light dispersion. It is also the hardest known material and is highly effective as an industrial cutting tool. The atomic number of carbon ($Z = 6$) is very similar to that of human tissue and is the main reason for the development of diamond radiation detection devices, since such devices will be useful in the medical and health physics fields. The diamond structure is chemically non-reactive, it will not react when placed in a hostile environment and will be non-toxic. It will be able to perform under varying conditions and temperatures, but will graphitize if heated above 700 °C in an oxygen environment. Most diamonds are insulating, a requirement for pulse counting radiation detectors. Pure diamonds consist solely of carbon in a sp^3 hybridized state, and the basic structure is described by the unit cubic cell of the diamond lattice (figure 2.3). Each cell contains eight atoms and has a length of 3.57 Å. The unit cell describes the perfect diamond structure – but all diamonds contain defects and impurities which affect its properties and lead to characterization of diamonds into different types.

Different concentrations of different impurities and defects cause diamonds to be classified into types, using a classification first proposed by Robertson et al (1934). The classification into type I and type II diamonds is related to their absorption in the infrared, visible and ultraviolet regions. Type II diamonds transmit well into the ultraviolet down to the absorption edge at 2200 Å, but type I diamonds show absorption starting at 3300 Å and increasing fairly rapidly at shorter wavelengths. The major diamonds types are as follows:

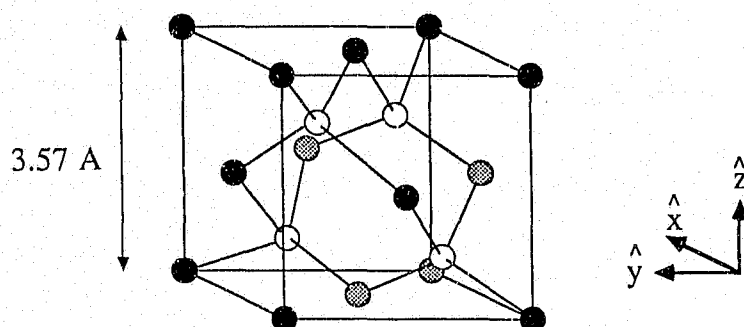


Figure 2.3. Unit cubic cell of diamond lattice.

Type Ia Characterized by appreciable amounts of the nitrogen impurity, the concentration of which can be determined from the strength of the infra-red absorption at $7.8 \mu\text{m}$. This class is presently split into A and B, depending on features appearing in the infra-red absorption spectra.

Type Ib Contains nitrogen atoms predominantly in the single substitutional form – the concentration can be measured using ESR techniques. Synthetic diamonds are of this type.

Type IIa Type II diamonds contain the least nitrogen and generally have the least impurities. Type IIa are insulating.

Type IIb Are semiconducting (*p*-type) due to the presence of boron and have a distinctive blue colouration, making them valuable as gems. Only a small proportion of type II diamonds are of type IIb.

2.3 Band structure

The band model describes electron energies and electron energy distributions, and is able to provide a simple and reasonably adequate explanation for the wide variety of electrical properties of solids (cf. for example Bube 1964, Ashcroft and Mermin 1976). An insulator such as diamond is described by the band model with a large energy gap (5.49 eV in the case of diamond). The valence band (below the gap) is fully occupied

by electrons and the conduction band (above the gap) contains no electrons (figure 2.4). The electrons are not free to move in the crystal and thus no electric current can flow – hence an insulator. If an electron is excited from the valence band to the conduction band, it becomes free to move as does the hole created in the valence band. Excitation takes place if energy is transferred to the electron, as is the case when the crystal is irradiated.

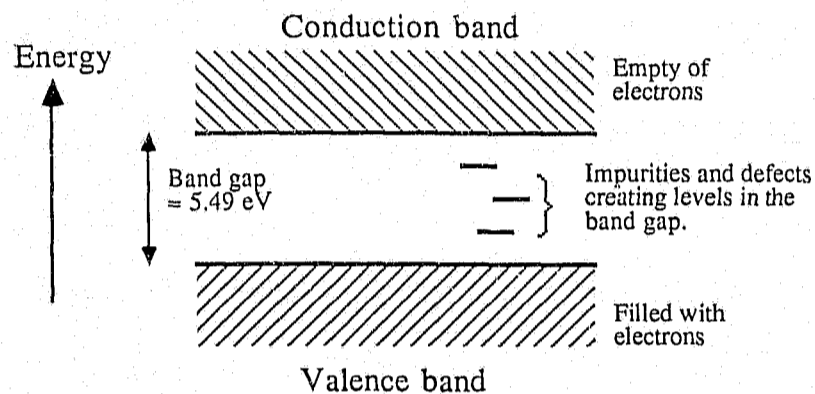


Figure 2.4. Band structure of diamond.

The presence of imperfections or defects in the crystal may affect the electronic behaviour by trapping charge carriers, causing charge carriers to recombine or doping the crystal so that it becomes semiconducting. An electron trap will temporarily capture a free electron from the conduction band and thermally excite the electron to the conduction band at a later stage. A hole trap acts in a similar manner by temporarily capturing a hole with subsequent thermal release to the valence band. The time between capture and release of the charge carriers depends on the trapping level energy and on the temperature of the crystal. A recombination centre causes recombination of a free hole and an electron – this either occurs between a hole and an electron captured at the recombination centre or between a free electron and a hole captured at the recombination centre. The process depends on the nature of the recombination centre, but both mechanisms will produce the same result. The energy released by recombination can be in the form of a photon usually in the visible region and, in such cases, the recombination centre is termed a luminescent centre. Alternatively the energy can be released in the

form of phonons, increasing the temperature of the crystal (this temperature increase is almost undetectable).

The difficulty in probing the electrical properties has resulted in only a few investigations of these properties of diamonds. The values used for the work described in this thesis (cf. sections 2.4 and 8.3) were obtained by Canali et al (1979). The values were obtained from diamonds used as pulse counting radiation detectors and were therefore similar to the diamonds described in this thesis.

2.4 The Hecht Function

The process describing how a charge carrier travels in a crystal under the influence of electric field was proposed by Hecht (1932) and described later for pulse counting diamond detectors by Hofstadter (1949) and Urlau (1960).

An assumption is made that the number of electrons trapped and/or recombined in a time t or a distance x is proportional the number of electrons present, thus

$$dN_e = -N_e \frac{dt}{\tau_e} \quad (2.6)$$

or

$$dN_e = -N_e \frac{dx}{W_e} \quad (2.7)$$

where N_e is the number of electrons,

τ_e is the lifetime, and

$W = \mu_e \tau_e E$ is the path length for electrons,

μ_e is the mobility, and

E is the electric field.

Solving this differential equation for N_0 free electrons created by the γ -ray interaction, yields

$$N_e = N_0 \exp(-t/\tau_e) \quad (2.8)$$

or

$$N_e = N_0 \exp(-x/W_e). \quad (2.9)$$

Integrating gives the total electron charge which is assumed to be created in a plane parallel to the electrodes a distance x_0 from the anode;

$$\begin{aligned} Q &= N_0 e \int_0^{x_0} \frac{1}{x_0} \exp(-x/W_e) dx \\ &= \frac{N_0 e W_e}{x_0} [1 - \exp(-x_0/W_e)]. \end{aligned} \quad (2.10)$$

And the total electron charge for electrons created homogeneously throughout the diamond of thickness s is

$$\begin{aligned} Q &= \frac{N_0 e W_e}{s} \int_0^s \frac{1}{s} [1 - \exp(-x_0/W_e)] dx_0 \\ &= \frac{N_0 e W_e}{s^2} \{s - W_e [1 - \exp(-s/W_e)]\}. \end{aligned} \quad (2.11)$$

A similar calculation applies to holes giving a total charge of

$$\begin{aligned} Q &= \frac{N_0 e W_e}{s^2} \{s - W_e [1 - \exp(-s/W_e)]\} \\ &\quad + \frac{N_0 e W_h}{s^2} \{s - W_h [1 - \exp(-s/W_h)]\}. \end{aligned} \quad (2.12)$$

This is the Hecht function and describes the charge collected at the electrodes if N_0 charge carrier pairs are created in a crystal. It has been mentioned in several reports (Hofstadter 1949, Urlau 1960, Vermeulen 1965, and Canali et al 1979) describing pulse counting diamond detectors, but no comparison of the Hecht function to experimental data has been made. This is because the space charge effect causes a reduced electric field in the diamond and charge collected as a function of the potential across the diamond does thus not obey the Hecht function.

Chapter 3. EXPERIMENTAL METHOD

3.1 Preparation of diamonds

The diamonds were synthesized and supplied by the de Beers Diamond Research Laboratory. They had been mechanically polished on two opposite and parallel (100) faces to allow for placing of electrical contacts, and an outer surface ($\approx 2\%$ by mass) had been removed by a chemical process involving surface oxidation (Burns 1989). The layer was removed because its conductivity was found in some cases to be higher than the bulk conductivity, producing a surface type conduction and a low resistance value for the diamond.

The masses and dimensions were recorded and the single substitutional nitrogen concentrations were measured using electron spin resonance (ESR) techniques. (cf. Chapter 7). The diamonds were usually about one cubic millimeter in volume and yellowish in colour. The yellow colour is the result of the nitrogen and diamonds with lower nitrogen concentrations were clearer and less yellow in appearance. Small metal inclusions were visible in most of the diamonds, but were more prominent in diamonds with lower nitrogen concentrations. The metal inclusions come from metal solvent/catalysts needed for the synthesis process and from gettering agents added to reduce the nitrogen concentration. A list describing each of the diamonds used appears in appendix A.

Scintillation counting measurements (cf. Chapter 6) and thermoluminescent measurements (cf. Appendix A) were carried out on most of the diamonds to determine something about their properties and to see if any correlations existed between scintillation, thermoluminescent and pulse counting measurements. These measurements had obviously to be done before the diamonds were ion implanted. (Thermoluminescent measurements are not discussed in this thesis, but spectra appear in appendix A for reference purposes. For details on thermoluminescence methods, results and models, refer to Nam (1989)).

To enable good electrical contacts to be made to the diamond, the polished faces were ion implanted (Prins et al 1987). The purpose of the implantation was to damage the surface layer, creating a conducting surface region which would enable a better electric contact to be made to the diamond. A more uniform electric field also results, as it is then formed between two plate like surfaces instead of between the points of attachment of the contacts.

Implantation was done with a Varian/Extrion model 200-20A2F ion implanter. The diamonds were masked to avoid implanting their sides. Masking was done by placing a metal foil, with a suitably sized aperture, over the diamond. The largest possible area of the polished face was exposed to the ion beam, but some of the surface still remained unimplanted due to the irregular surface shapes. Another method allowing the whole face to be implanted was also employed: the diamonds were mounted in 'duroc', a plaster of Paris like substance, so that only the polished face was exposed. Before implantation the diamonds were cleaned by boiling them in an acid solution of 1 part HNO_3 , 3 parts HClO_4 and 4 parts H_2SO_4 for 15 to 20 minutes. If the surface to be implanted was not clean, then dirt on the surface would be implanted along with the ions during the implantation process.

The faces were implanted with either boron (^{11}B) or carbon (^{12}C). Carbon was implanted at three different energies to create a uniform depth distribution. The diamond was heated to 100°C and implanted with with a dose of 3×10^{16} ions $\cdot\text{cm}^{-2}$ at 120 keV, 2×10^{16} ions $\cdot\text{cm}^{-2}$ at 60 keV and 1×10^{16} ions $\cdot\text{cm}^{-2}$ at 30 keV. Any graphite which had formed during implantation was removed from the surface by cleaning the diamond again in the acid solution. An initial implant with boron was done in a similar way to the carbon implants. The effect was however the same, a damaged layer was created resulting in a Schottky ohmic contact. Later boron was implanted to create a *p*-doped surface layer, using a method discovered by Prins (1989a, 1989b). The diamond was first cleaned in the acid solution and then implanted with 3×10^{16} ions $\cdot\text{cm}^{-2}$ at 35 keV while at 150°C . It was annealed at 1200°C for 10 minutes, allowing the boron atoms to diffuse and recombine with vacancies and thus creating a *p*-doped region below the damaged layer. The diamond was then boiled in the acid solution for about two hours to remove the damaged surface layer, leaving a boron doped layer characterized by a slightly bluish tinge in the colour.

When the diamond was implanted with boron and carbon on opposite faces, boron implantation was done first - otherwise the long acid cleaning to remove the damaged layer would also have removed the carbon implanted surface region.

Thin gold wires which had been flattened at the end to ensure a larger contact area and thus a stronger contact, were attached to the two implanted surfaces with a silver loaded epoxy adhesive. The diamond was held in a vice and the gold lead was manipulated and held by a micromanipulator. The epoxy was applied to the bottom of the flattened lead which was then moved into place on the diamond surface. Excess epoxy was removed, and the contact was heated by an infra-red heater to 180 °C for 12 to 24 hours to dry the epoxy. All the above manipulation was done under a microscope because of the small size of the contact and the need for precision. The contacts formed were strong enough to support the diamond, but tended to disintegrate if heated above 300 °C.

Three natural Iia diamonds were also tested for comparison purposes. They had been mechanically polished on opposite parallel (100) faces and were not ion implanted. The leads were attached as described above with the silver loaded epoxy adhesive. These natural diamonds are also listed and described in appendix A.

3.2 Electronic circuitry

The electric circuit to which diamonds were connected for the pulse counting measurements is similar to conventional circuits used for obtaining pulse height spectra, and is shown schematically in figure 3.1. Initially, a special circuit was designed and built (Grobelaar 1988), because the pulses emitted from the diamond were very small and a large amplification was necessary.

The circuit contained a preamplifier, amplifier, a pulse counter with variable discriminator setting, and a high voltage power supply (circuit diagrams are included in appendix B). The diamond was mounted directly onto the preamplifier's circuit board so that capacitance between the leads from the diamond would be at a minimum. The preamplifier was separate and joined to the rest of the circuit by long cables. This allowed the preamplifier and diamond to be placed in a radiation monitoring position, and the rest of the circuit in a radiation safe area.

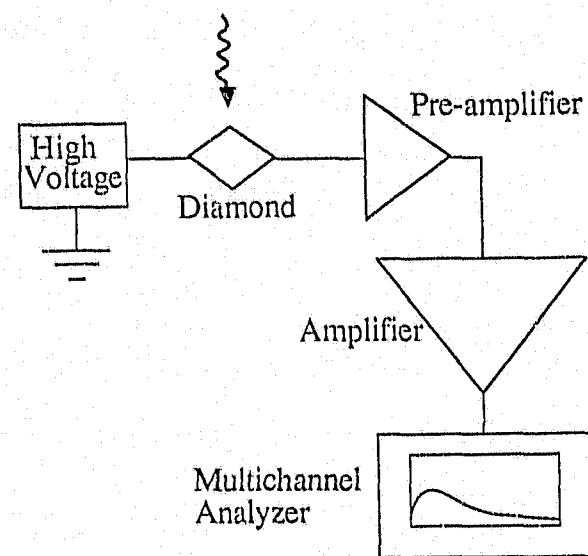


Figure 3.1. Schematic diagram of circuit used for pulse counting measurements.

Radiation interacting with the diamond releases charge carriers by ionization. Electrons are excited from the valence band into the conduction band and are free to move, as are the holes produced in the valence band. The high voltage across the diamond creates an electric field which sweeps the electrons to the positive contact and the holes to the negative contact. This produces a small electric pulse, which is amplified by the preamplifier and the amplifier, and then counted and recorded. The energy deposited by the radiation is proportional to the number of charge carriers released. Thus the size of the pulse should be proportional to the energy deposited by the incident radiation.

The counter with variable discriminator setting was disconnected as it produced feedback pulses in the main amplifier. The result was a peak which appeared in the pulse height spectrum, and was at first mistaken for the full γ -ray energy peak. The output from the amplifier was instead connected to a Canberra series 20 multichannel analyzer (MCA) which could record in either pulse height analysis or multichannel scaling modes. Recording the spectra on the MCA gave information about the size and distribution of pulses, which would not be obtained from a simple counter. The

spectral data was transferred from the MCA to a personal computer for storage and data processing. The high voltage power supply was able to switch between negative and positive voltages in less than a second. This feature was used in recording some spectra to obtain information about the space charge effect. The power supply was sometimes disconnected and replaced by an Ortec 456 high voltage power supply which was more stable and had a larger voltage range.

A typical ^{137}Cs γ -ray spectrum appears in figure 3.2. The x-axis is in channels which are a measure of the pulse height. The y-axis displays the number of pulses in each channel and is in a logarithmic scale because of the shape of the spectrum. Two distinct regions can be seen. The low energy region which has a very high count rate is due to electronic noise. It remains unchanged when no radiation is incident on the diamond (this background spectrum is indicated by the dotted line in figures 3.2 and 3.3). The high energy region which is not present in the background spectrum is produced by pulses created when the γ -rays interact with the diamond. The shape is exponential and not the expected Compton shape (figure 2.2). This shows that the pulse height is not directly proportional to the energy deposited by the incident radiation. No full γ -ray energy peak appeared in the spectrum and so no energy calibration was possible, the spectrum is thus plotted as a function of channels.

A region of interest (ROI) was defined on the MCA which integrated all the pulses in this region. The ROI included all the channels above the background region, and the integrated number of pulses was used as a measure of the radiation dose rate. A small background count rate of about 10 counts per 100 seconds usually occurred in the ROI and imposed a limit on the minimum dose rate that could be measured. It was thus not possible to measure radiation dose rates producing less than about 15 counts per 100 seconds. It also meant that lower dose rates could not be measured by counting pulses for longer periods of time, thus most spectra were recorded for a 100 second live time period. Recording for shorter periods would have meant larger statistical errors.

The periods used in the multichannel scaling mode were set with dwell time of 1 second per channel and measuring over 512 or 4096 channels (total times of $8\frac{1}{2}$ minutes or 1 hour and 8 minutes). For longer periods a maximum dwell time of 4 seconds was set and measured for all 4096 channels, - a total time of $4\frac{1}{2}$ hours.

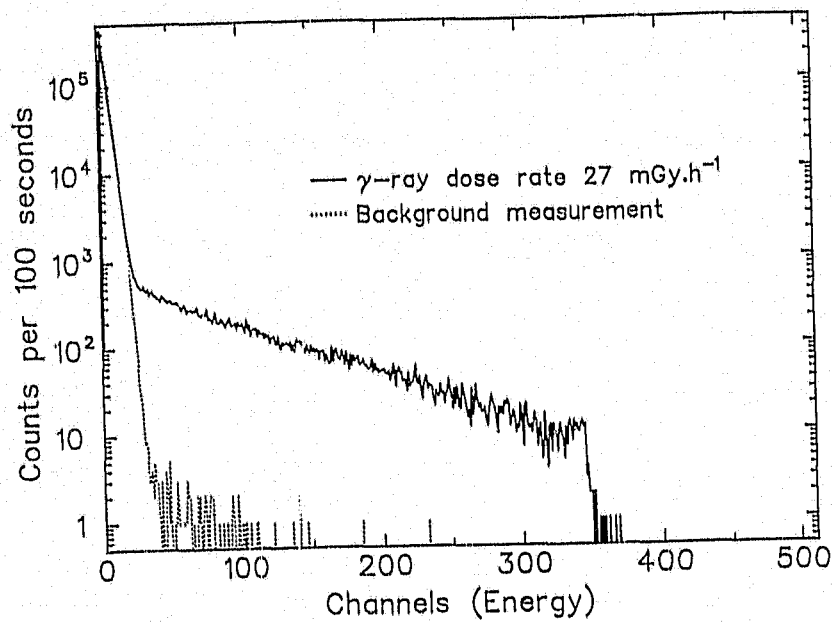


Figure 3.2. A typical ^{137}Cs γ -ray spectrum, using a synthetic diamond detector and custom built electronics (maximum pulse height is the result of amplifier saturation). Diamond: Suite 2.

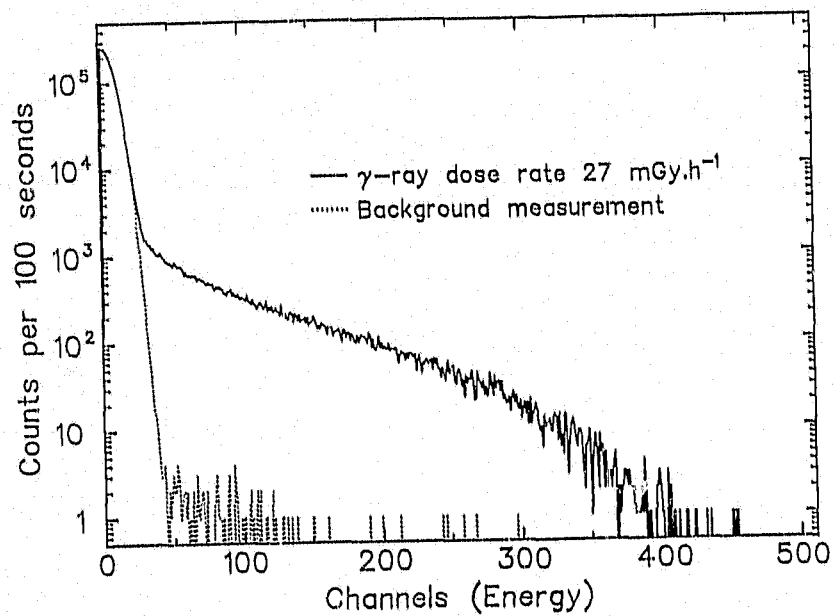


Figure 3.3. A typical ^{137}Cs γ -ray spectrum, using a synthetic diamond detector and conventional electronics. Diamond: Suite 2.

For diamonds emitting large pulses it was possible to use conventional pulse counting circuitry. The custom built circuit differed by not having negative feedback in the first amplification stage, producing a lower input impedance and thus larger pulses overall. Differences between the two circuits also occurred in the way the diamond, high voltage power supply and load resistor were connected (figure 3.4). This would not effect the pulses produced, but pulses from the conventional circuit should have a slightly higher signal to noise ratio. It was not possible to alter the amplification on the custom built circuit (electrical components would have to be changed). Saturation of pulse height occurred in some cases (cf. figure 3.2), but the pulses were then large enough for conventional circuitry to be used. The conventional circuitry consisted of an Ortec 109A preamplifier, a Canberra 1413 amplifier, an Ortec 456 high voltage power supply and the Canberra series 20 MCA. Holders were made so that the diamond could be mounted as close to the preamplifier as possible. Similar spectral responses were obtained from both circuits (compare figures 3.2 and 3.3), showing that both circuits worked equivalently. The custom built circuit was used when the pulses were very small and a large amplification was necessary; when large pulses were produced the conventional circuitry was used.

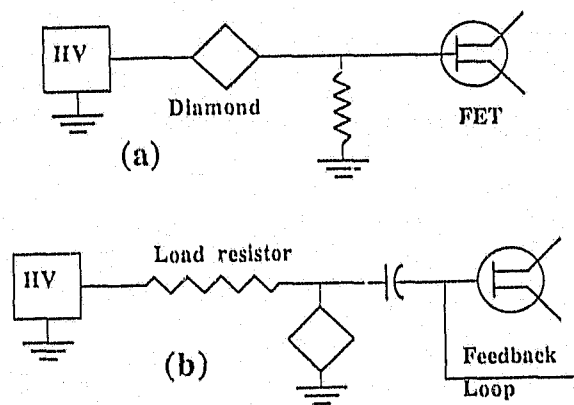


Figure 3.4. Circuit diagrams for connections between diamond, high voltage power supply and load resistor - (a) custom built circuit, (b) conventional surface barrier detector circuit.

As the potential across the diamond increases, more charge carriers are collected at the contacts. Saturation eventually occurs when all the charge carriers are collected. A plot of the count rate versus applied potential (figure 3.5) shows that in the voltage region used for the experiment (100 - 1000 V) saturation of the count rate did not always occur. Thus for some measurements the count rate was dependent on the applied potential. Potentials greater than 1000 V were not possible because of electrical breakdown and high leakage currents. It was also not possible to use some diamonds because their resistance was too low and large currents flowing through the diamond made it inoperable as a pulse counter.

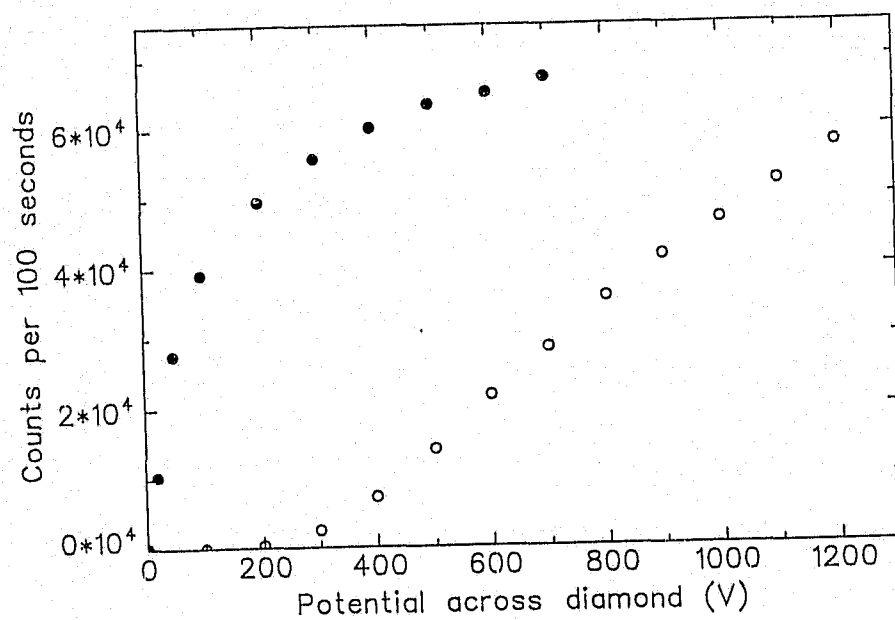


Figure 3.5. Plot of count rate versus potential. Open circles, diamond not implanted, no saturation occurs below 1200 V. Solid circles, diamond with boron and carbon implants, saturation begins to occur at 600 V.

For measurements where it was necessary to keep the diamond in the dark, the holder was covered with black insulation tape. Attenuation of the γ -rays by the tape was negligible. The diamond was usually kept in the light tight holder, because if exposed to light it would have needed to be pre-irradiated again. It was also kept in the dark during pre-irradiation.

3.3 Radiation sources

Most measurements were carried out using a ^{137}Cs γ -ray radiation source. The source had a strength of 100 mCi and produced γ -rays with an energy of 661.2 keV. Dose rates were calibrated for distances from the source and, since ^{137}Cs has a half life of 30.2 years, the change in dose rates between spectra measured at different times is negligible. Different doses were incident on the diamond by placing it and the preamplifier at various distances from the source. This allowed a dose rate range of $100\ \mu\text{Gy}\cdot\text{h}^{-1}$ to $30\ \text{mGy}\cdot\text{h}^{-1}$ to be measured. For low dose rates an attenuator was used reduced the dose rate by a factor of 100. This gave a minimum dose rate of $1\ \mu\text{Gy}\cdot\text{h}^{-1}$, which was only slightly higher than the laboratory background of 0.5 to $0.7\ \mu\text{Gy}\cdot\text{h}^{-1}$. Normal background levels are usually $\approx 0.1\ \mu\text{Gy}\cdot\text{h}^{-1}$.

A ^{60}Co γ -ray source was used for the pre-irradiation of diamonds and for some pulse counting measurements. The ^{60}Co source had a strength of 3000 mCi and has a half life of 5.27 years. It produces two γ -rays of energy 1.173 and 1.332 MeV, both with equal intensity as they are in a cascade.

X-rays source from a X-ray spectrometer, and two conventional radiation therapy X-ray sets were used to investigate the response of the diamond to different energies and different dose rates. The dose rates from the ^{60}Co and from the X-rays were measured by a 2502/3 Farmer Dosimeter. The values were measured in units of air exposure (roentgen(R)) and converted to the diamond absorbed dose (gray(Gy)). All measurements of γ -ray and X-ray sources were done at room temperature and at atmospheric pressure.

Measurements of α -particles were done using ^{241}Am α -particle foil sources. ^{241}Am has a half life of 433 years and produce α -particles of energy 5.486 MeV. Since the α -particles lose their energy after traveling through only a few centimeters of air, these measurements had to be done in a vacuum. For this purpose the diamond and α -particle foil source were placed in a vacuum chamber and the preamplifier was placed outside the chamber, with the leads from the diamond to the preamplifier being made as short as possible.

Chapter 4. PULSE COUNTING RESULTS

4.1 Introduction

The ^{137}Cs pulse height spectra measured with the diamond detectors, were exponential in shape and did not contain any Compton edge or full γ -ray energy peak (figures 3.2 and 3.3). The absence of a peak is understandable in terms of the diamond's small size. The probability that a 661.2 keV γ -ray photon will lose its total energy to the diamond by photoelectric absorption is negligible in comparison to the probability of a Compton scattering event occurring (compare cross sections at 661.2 keV, figure 2.1). In Compton scattering, however, only a fraction of the energy is lost per Compton interaction. The total energy is absorbed by several Compton interactions followed by photoelectric absorption. The probability of Compton scattering in diamond is small, only 2.7 % of the 661.2 keV γ -rays will interact with a one millimeter thick diamond ($0.35 \text{ g}\cdot\text{cm}^{-2}$), and the probability of multiple scattering of a single γ -ray is less than 2.7 % of the original 2.7 %. Thus the probability of observing a pulse corresponding to the full γ -ray energy is extremely small, and the spectrum should contain only the rectangular shaped Compton region - which was not observed in any spectrum. The recorded pulse height distributions, being different to those expected from Compton scattering, indicate that the processes occurring within the diamonds are not all accounted for. Possible reasons explaining the pulse height distribution are discussed in chapter 8.

The number of pulses (i.e. counts in the ROI) recorded for a fixed time (usually 100 seconds) was used as a measure of the γ -ray radiation dose rate, and enabled the diamond counter's response as a radiation detector or dosimeter to be investigated.

With the early experiments the count rate was found to vary as a function of time (figure 4.1). When the high voltage was switched on and pulses were recorded, the pulse counting rate decreased until a saturation value was reached. The shape of the pulse height spectrum remained unchanged, but the average pulse height was reduced and fewer pulses occurred in the ROI (figure 4.2).

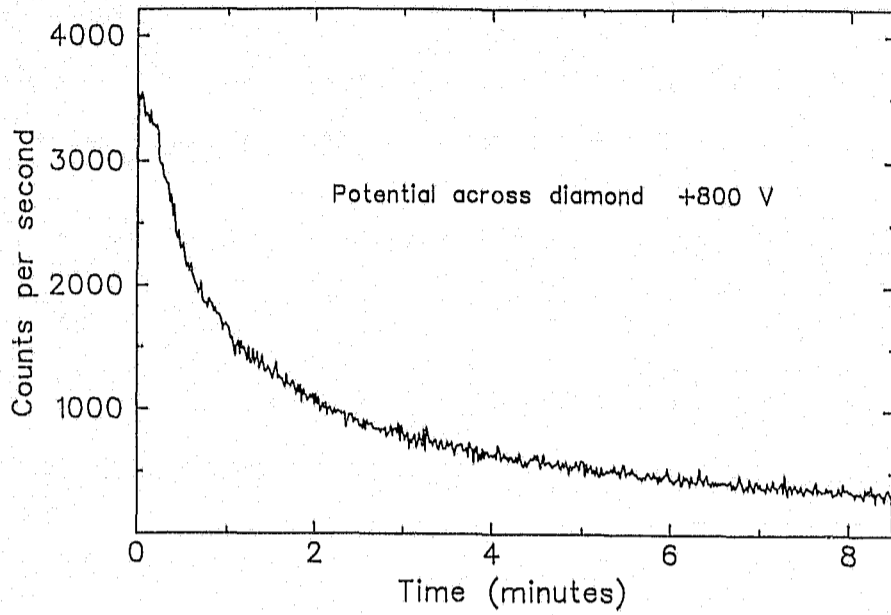


Figure 4.1. Pulse counting rate measured as a function of time.
Diamond: Original 691.

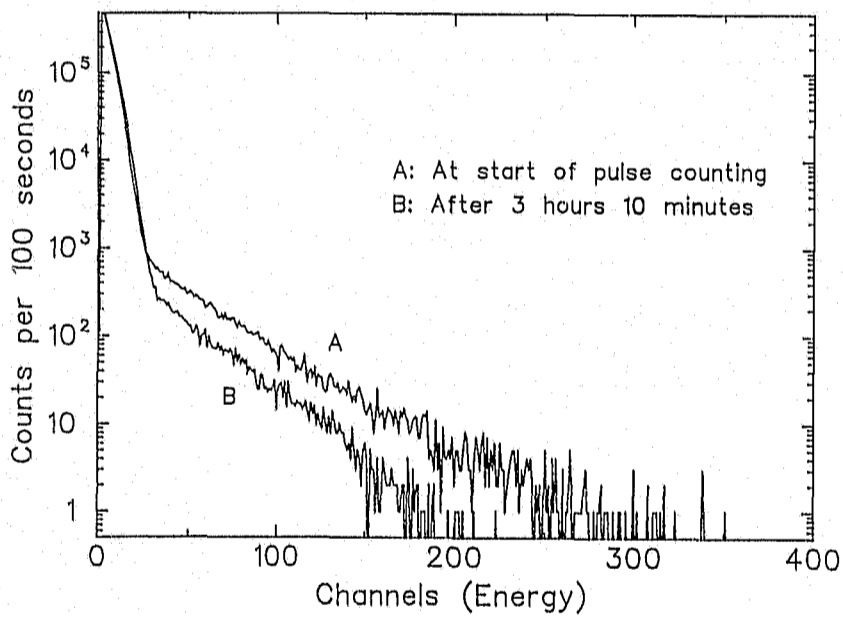


Figure 4.2. Initial pulse height spectrum and pulse height spectrum recorded three hours later. Diamond: D21.

A decreasing count rate with time has been seen in almost all the investigations in which diamond has been used as a pulse counter (Willardson 1950, Cotty 1956a, Cotty 1956b, Urlau et al 1961, Champion and Kennedy 1956, Afanas'eva and Konorova 1964, and Vermeulen and Nabarro 1967b). The decrease results from the occurrence of space charge inside the diamond. The electrical contacts form a barrier which the charge carriers must cross, and those that do not cross the barrier are trapped close to the contact, creating an excess of charge carriers (Hofstadter 1949). Electrons are trapped close to the positive contact and holes are trapped close to the negative contact, producing an electric field which opposes the electric field created by the high voltage. As the space charge increases, the effective electric field is reduced, causing a lower collection efficiency for charge carriers, smaller pulses and thus fewer integrated counts in the ROI (figure 4.2).

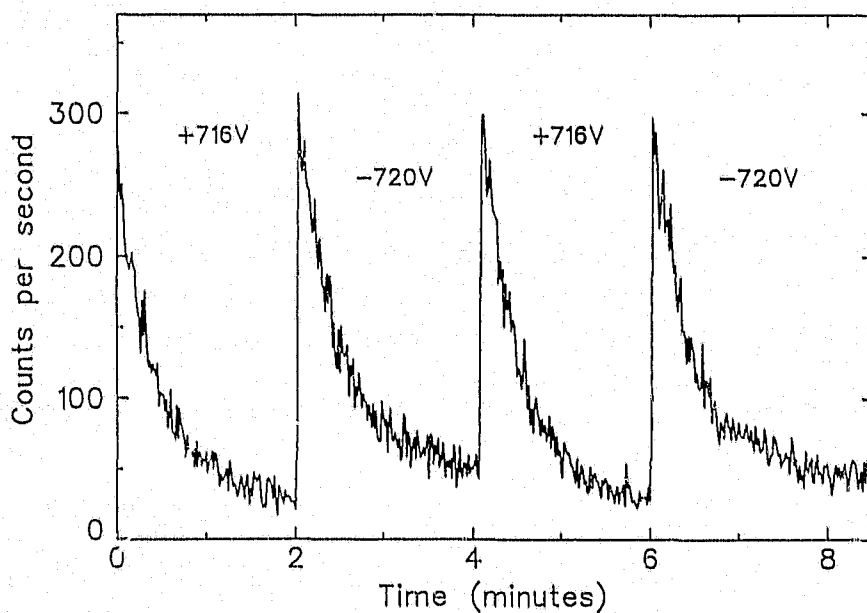


Figure 4.3. Count rate of a diamond counter, with polarity of high voltage across diamond switched at two minute intervals. Diamond: SIN 3.

When the high voltage across the diamond was switched off, pulses appeared - but with opposite polarity to those occurring when the high voltage was switched on. This indicates that charge collection occurred because of the space charge field, an effect which has also been observed by Willardson (1950). The pulses reduced in size as the

space charge dissipated and were no longer visible after a few minutes. The space charge effect can clearly be observed in figure 4.3, where the polarity of the high voltage was switched at two minute intervals. Initially the count rate decreased as the space charge developed, but, when the polarity was switched, the immediate space charge field no longer opposed the high voltage field and a high count rate resulted. The space charge again developed rapidly, opposing the potential field and reducing the count rate. The slight difference in the saturation count rate between negative and positive polarity (figure 4.3) is believed to result from an unsymmetrical trapping level distribution in the diamond.

To reduce the space charge effect, the polarity of the high voltage can be switched at regular intervals (Wouters and Christian 1947, McKay 1948, Hofstadter 1949a). The custom built high voltage power supply and pulse height circuit were initially designed with this in mind but were unsuccessful since the switching produces many noise pulses, no counting was possible during switching and the high voltage was not always of the same value. Switching only works to a limited extent, it is not an acceptable way around the space charge problem and was thus not considered a solution. Another method of reducing the space charge is to expose the diamond to red light. The light releases trapped charge carriers and so reduces the space charge (Chynoweth 1947, Willardson and Danielson 1950, Vermeulen and Nabarro 1967a, 1967b). Pulse counting measurements were performed whilst the diamond was illuminated with light, but large photoconduction currents made the diamonds inoperable as effective pulse counters. (The effect of light is discussed in detail in chapter 5). The above methods are ways of reducing the space charge, but are not ways of removing the cause of space charge (i.e. the contacts that form a barrier for the charge carriers to cross). The correct approach to solving the space charge problem is to create electrical contacts that do not form a barrier for the charge carriers to cross. The charge carriers are then free to move through the crystal to the conducting leads and trapped space charge will not arise.

The space charge effect was found to differ from diamond to diamond and was also found to differ depending on the type of contacts used. Because of the space charge effect, pulse counting results were time dependent, thus causing problems with repeatability. Initially for consistency, measurements were carried out immediately after switching on or after a saturation count rate had been reached.

4.2 Different electrical contacts tested

Several different methods of making contacts to the polished diamond faces were investigated. The first and simplest method investigated consisted of applying leads to the cleaned polished opposite faces with silver loaded epoxy adhesive. Diamonds with these contacts displayed decreasing count rates because of the space charge effect.

The initial method of improving the contacts to reduce the space charge effect involved ion implanting both surfaces with carbon (Prins et al 1987). An additional advantage is that the implanted regions form plate-like areas, producing a more uniform electric field throughout the diamond. The leads which were initially attached to just the polished faces with silver loaded epoxy adhesive were removed, both surfaces were cleaned, ion implanted with carbon and new leads were attached. Comparisons of a diamond with and without carbon implanted contacts (figures 4.4 and 4.5), indicate that a higher count rate occurs and the space charge effect is reduced when the surfaces are implanted with carbon. The carbon ion implantation improves the contact, but the space charge effect remains.

Other methods of making electrical contacts were tested. The polished surfaces were laser-scribed and contacts applied with the silver loaded epoxy adhesive. Gold evaporated on to the polished surfaces by Drukker International was also tested as a method of making contacts to unimplanted, laser-scribed and carbon implanted surfaces. All these contacts were unsuccessful as the space charge effect was noticeably present.

It was finally decided to employ a method similar to that used by Konorova and Kozlov (1971), who claim to have suppressed the space charge effect by creating a 'hole injection contact'. They report that their contact, connected to the positive potential, was made by creating 'a surface layer of boron-doped diamond' and 'an electrode made of silver paste' (Kozlov and Konorova 1971, Kozlov et al 1975). The opposite contact was made by evaporation of gold on to the diamond surface and was connected to the negative potential. Diamonds with these contacts were said to maintain a constant radiation counting rate and to display good energy resolution for detection of α -particles (Kozlov and Konorova 1971, Kozlov et al 1975).

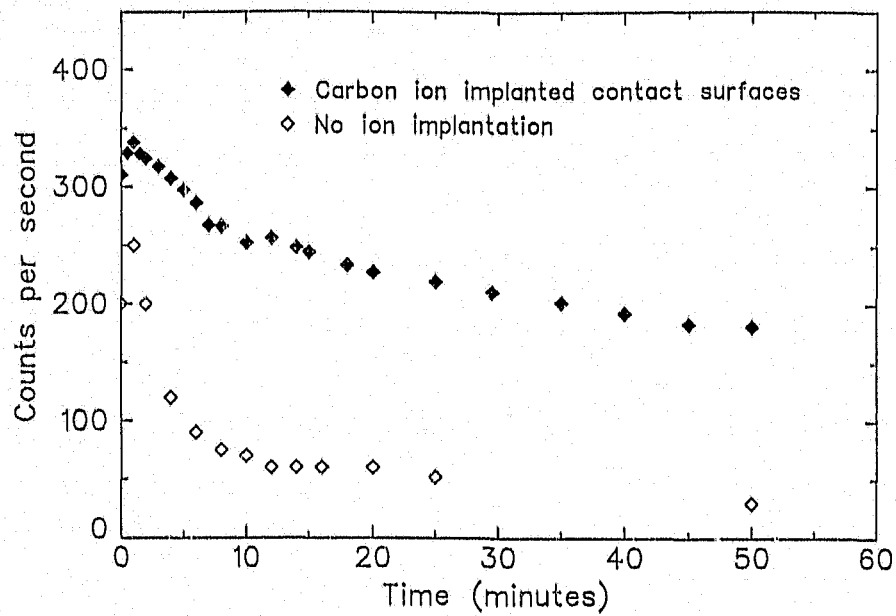


Figure 4.4. Count rate as a function of time, showing the effect of ion implanting both polished surfaces with carbon. Diamond: CoFe stone 5.

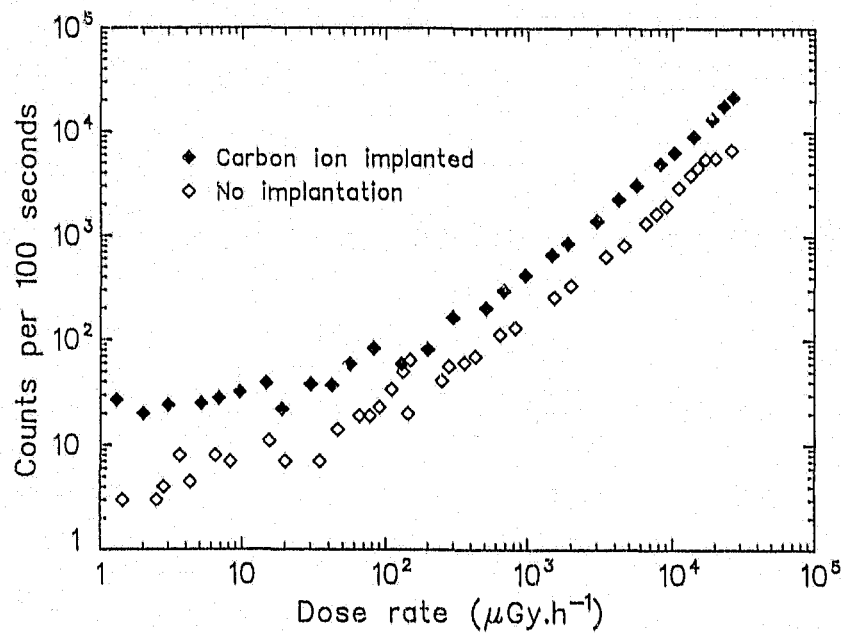


Figure 4.5. Count rate as a function of dose rate, showing the effect of ion implanting both polished surfaces with carbon. Diamond: CoFe stone 5.

4.3 The boron *p*-doped contact

Boron ion implantation was used to create a *p*-doped surface layer for one of the polished faces. The method used was suggested by Prins (1989a, 1989b) and is described in chapter 3. This *p*-type surface layer was used as the positive contact, in the same way as the positive contact described by Konorova and Kozlov (1971). The opposite polished face, used as the negative contact, was ion implanted with carbon, in the same way as the previous carbon ion implanted contacts. With these contacts no decrease in the pulse counting rate was observed (figure 4.6). The contacts thus successfully eliminated the development of space charge. If the polarity was reversed, a space charge related decrease was observed (figure 4.6), indicating that the contacts are voltage polarity dependent. Therefore with the correct polarity and because the count rate remains constant with these boron-carbon contacts, the measurements were repeatable no matter when they were carried out.

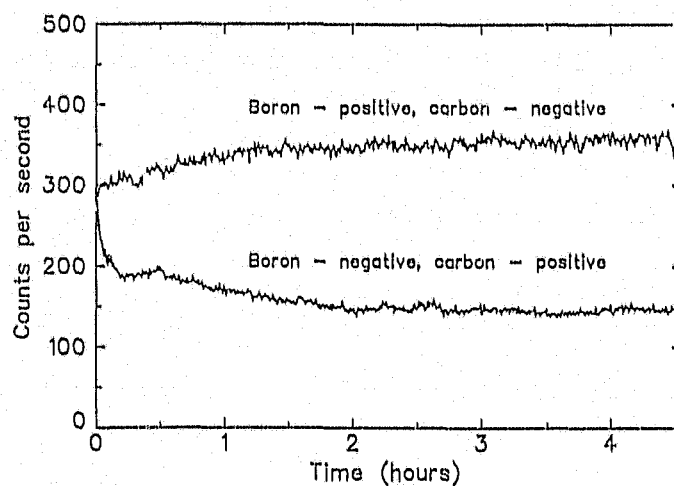


Figure 4.6. Count rate as a function of time for diamond with boron *p*-doped and carbon ion implanted contacts. Diamond: Suite 2.

An initial increase was observed in the counting rate when the diamond was first used after pre-irradiation (figure 4.6). The increase was not observed at any other stage (figure 4.12), and the count rate remained at the high value reached after the initial increase. No increase was observed if the diamond was tested several hours after the pre-irradiation. This increase is discussed in further detail in chapter 5. If the pulse counting measurement was stopped after the initial increase, and the diamond was left with no voltage applied and no radiation or light incident on it for a period of at least

a day, a small space charge decrease (less than 5 %) was observed (figure 4.12). The small space charge decrease was not initially observed since it has a smaller effect and becomes insignificant in comparison to the initial increase.

Two boron *p*-doped contacts were tested on diamond suite 2 no. 3 (figure 4.7). The pulse counting rate displayed a small initial decrease, indicating that space charge did develop (figure 4.7). The space charge effect was less significant than that observed for two carbon implanted contacts, but was more significant than that observed for diamonds with a boron *p*-doped and a carbon ion implanted contact.

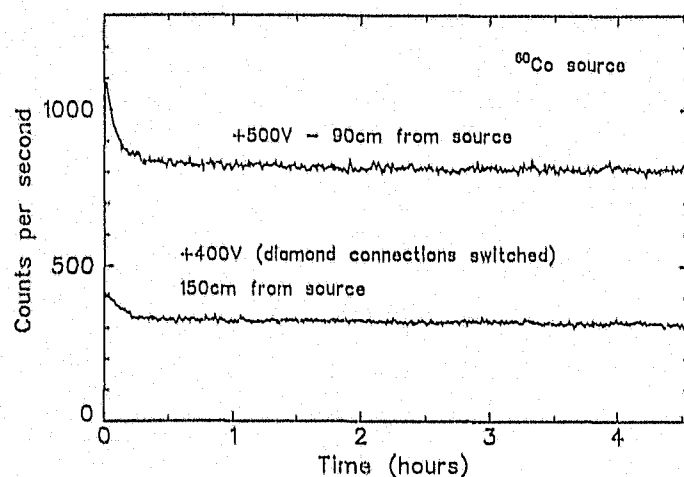


Figure 4.7. Count rate as a function of time for diamond with two boron *p*-doped contacts. Diamond: Suite 2 no. 3.

4.4 Pre-irradiation

For diamonds with low paramagnetic nitrogen concentrations (< 60 ppm), it was found that pre-irradiation with a γ -ray dose greater than 10 Gy initiated a much higher count rate and reduced the effect of the space charge (figure 4.8). The 'pre-irradiation' effect also occurred if the diamond was left in the radiation field of a γ -ray or X-ray source whilst not exposed to light (figure 4.9). The count rate was initially very small, but increased to a saturation value as 'pre-irradiation' occurred. The pre-irradiation did not however affect synthetic diamonds with paramagnetic nitrogen concentrations greater than 60 ppm, and all diamonds primed by pre-irradiation could be returned to the unprimed state by exposure to ambient light for a few seconds (figure 4.10).

Similar increases in response by irradiation have been observed by Keddy (1988) for low nitrogen synthetic diamonds used to measure the d.c. conduction response to radiation, and by Burgemeister (1982) who also used low nitrogen synthetic diamonds and a natural IIa diamond to measure the d.c. conduction response to radiation.

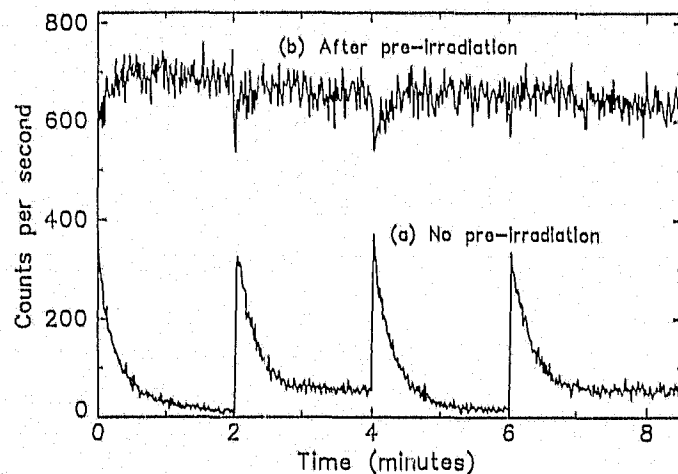


Figure 4.8. Count rate for diamond with polarity of high voltage switched at two minute intervals. Diamond: SIN 3.

It is suggested that the 'pre-irradiation' increase in response is due to the filling of trapping levels within the diamond. If the trapping levels are not initially filled, they trap the charge carriers from the radiation induced pulses, reducing the size of the pulses and, because of the discriminator setting, cause fewer pulses to be counted (i.e. to occur in the ROI). The slow rise in the count rate (figure 4.9) occurs as the trapping levels become filled and less trapping results in a higher count rate. Exposure to light causes these trapping levels to be depopulated, i.e. the diamond is returned to the unprimed state. It is believed, after testing, that there is only a single trapping level, its energy was measured and is discussed chapter 5.

A low nitrogen diamond (Suite 2, 7 ppm nitrogen) which was pre-irradiated and had a boron *p*-doped and a carbon ion implanted contact maintained the same count rate for a period of a month (figures 4.11 and 4.12). Indications are that diamonds of this type should maintain the same count rate indefinitely, so long as they are not exposed to light or heated sufficiently to depopulate the trapping level or levels.

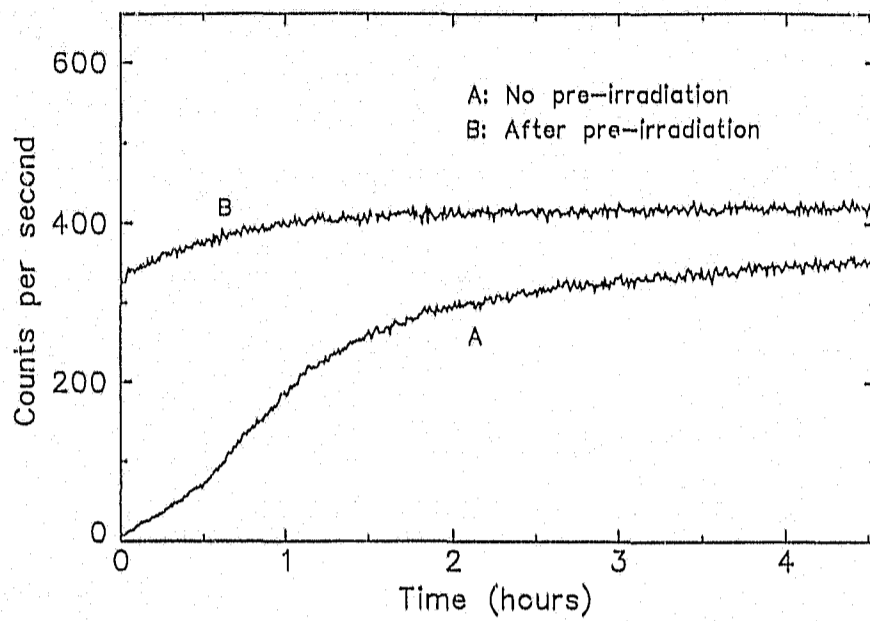


Figure 4.9. Diamond with a boron *p*-doped contact, not exposed to light. (A) 'Pre-irradiation' performed whilst counting, and (B) measured after a 10 Gy γ -ray pre-irradiation dose. Diamond: Suite 2.

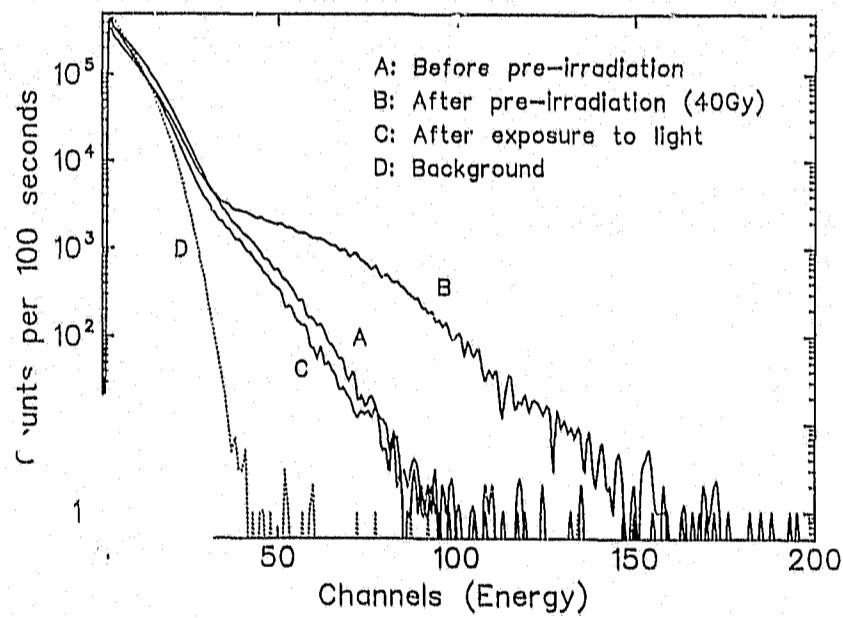


Figure 4.10. Pulse height spectra showing the effect of pre-irradiation and the effect of exposing a pre-irradiated diamond to light. Diamond: SIN 3.

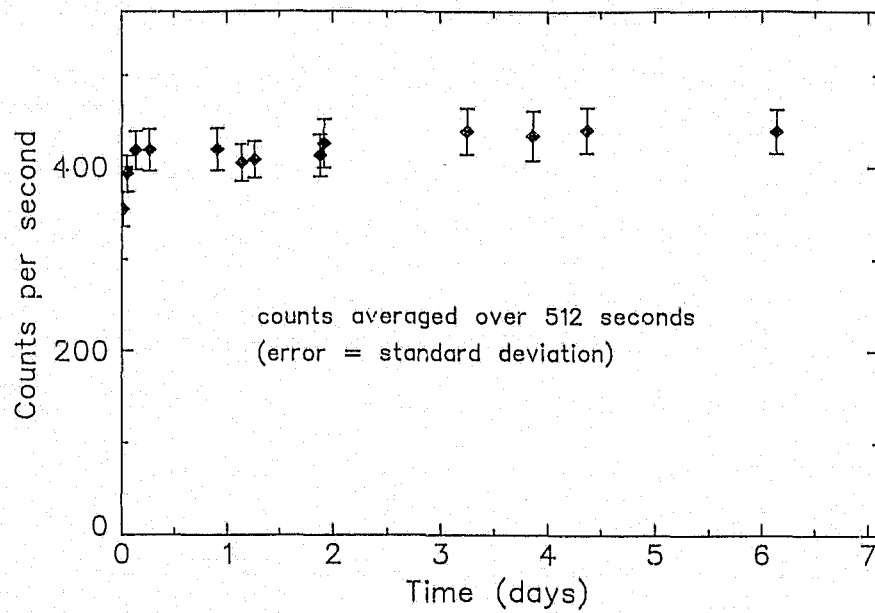


Figure 4.11. Count rate for pre-irradiated diamond with a boron *p*-doped and a carbon ion implanted contact, measured once or twice a day for seven days. (Between the measurements no potential was applied across the diamond, and the diamond was not exposed to any radiation). Diamond: Suite 2.

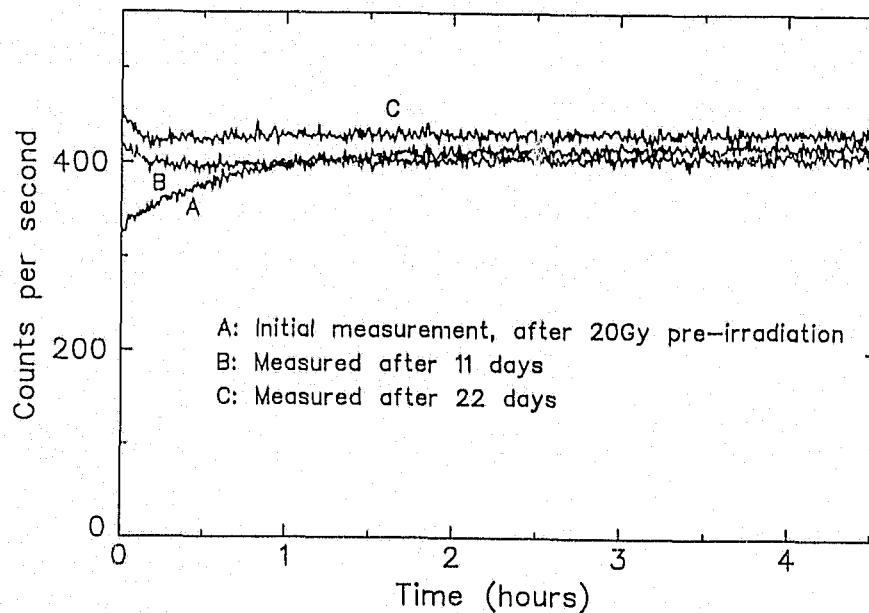


Figure 4.12. Pulse counting measurements performed after pre-irradiation and after two eleven day periods. (Between the measurements no potential was applied across the diamond, and the diamond was not exposed to any radiation). Diamond: Suite 2.

4.5 The effect of using different radiation sources

The pulse height spectra of ^{137}Cs and ^{60}Co γ -ray sources and low energy X-ray sources were measured (figure 4.13). These spectra are different in shape but are similar in so far that the shapes are exponential in first approximation. Differences occur because of the different energies and different energy distributions of the γ - or X-rays. The ^{137}Cs source produces a single γ -ray with an energy of 661.2 keV, and the ^{60}Co produces γ -rays of energy 1.173 and 1.332 MeV, both with equal intensity. The X-rays range from zero to the maximum X-ray energy for the particular source and the intensity varies over this range. The measured half value layers were used to interpret the effective energies of the two 'hospital' X-ray sources. The energy absorbed by the diamond will depend on the energy absorption cross section of diamond for the particular energy. It was not possible to calibrate the spectra in terms of energy because no peak appeared from which a correlation could be obtained. But it can be seen from figure 4.13 that the average pulse height increases with increasing radiation energy. The relationship between the slope of the semi-log pulse height spectral representation and the radiation energy was investigated and is described in chapter 8.

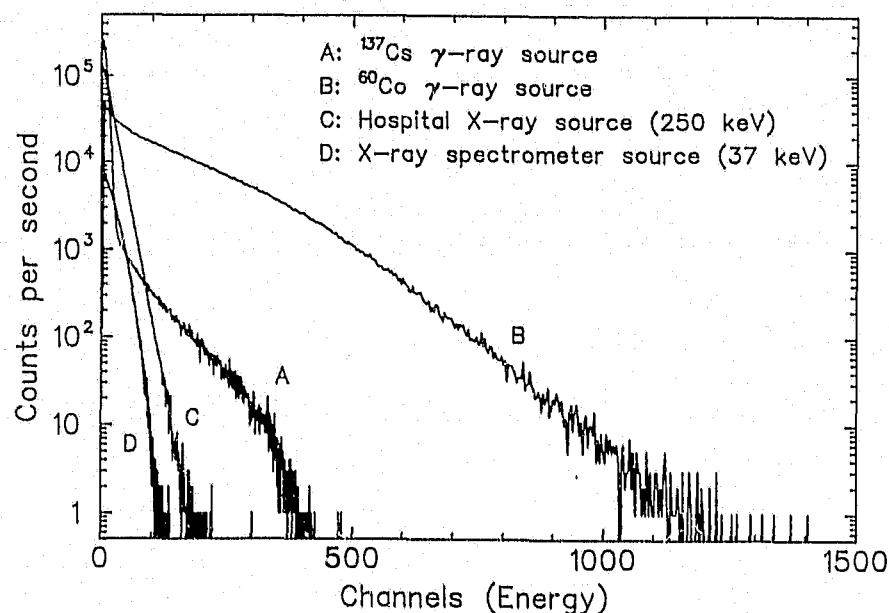


Figure 4.13. Pulse height spectra of various radiation sources, using pulse counting diamond detector. (Maximum X-ray energies are given in brackets). Diamond: Suite 2.

4.6 Alpha particle measurements

The response of the diamond pulse counting detectors to α -particles was investigated. It was hoped that a peak corresponding to the α -particle energy would be observed in the pulse height spectrum as reported by Konorova and Kozlov (1971), Kozlov et al (1975), Nava et al (1979), and Canali et al (1979).

The measurements were performed in a vacuum of 6×10^{-2} mbar (Torr), because α -particles are attenuated in air. The α -particles were obtained from a ^{241}Am foil source and had an energy of 5.486 MeV. Most of the diamonds were tested as α -particle detectors, and all were able to detect the α -particles. The pulse height spectra were again exponential in shape and no peaks corresponding to the full α -particle energy were observed (figure 4.14).

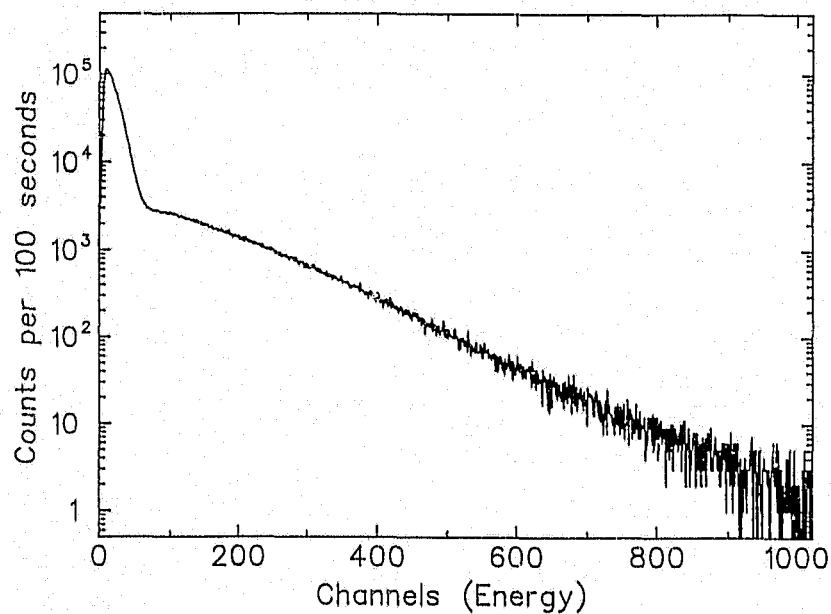


Figure 4.14. Pulse height spectrum of ^{241}Am α -particles incident on polished face between contacts. Diamond: Suite 2 no. 4.

The diamonds were irradiated from all possible directions (i.e. α -particles incident on both contact faces and on the diamond surfaces between the contacts), but no changes were observed in the shape of the spectra. It was thought that attenuation of the α -particles by the contacts or poor charge carrier collection because of distorted electric

fields at the rough diamond surfaces between the contacts may have been responsible for the shape of the pulse height spectrum. Two synthetic diamonds (7 ppm and 130 ppm single substitutional nitrogen concentration) were specially prepared for α -particle detection. A flat face was polished between the two contact faces so that charge carriers created by α -particles incident on this face would be collected by a uniform electric field. The pulse height spectra of α -particles from these diamonds were also exponential in shape and no full α -particle energy peak was observed (figure 4.14).

4.7 Dose rate measurements

The number of counts (pulses) in the ROI of the pulse height spectrum was used as a measure of the radiation dose rate. The relationship (figure 4.15) was linear over five orders of magnitude. Minimum dose rates of approximately $1 \mu\text{Gy}\cdot\text{h}^{-1}$ were recorded, only a factor of 10 above normal background radiation levels of $0.1 \mu\text{Gy}\cdot\text{h}^{-1}$. The minimum dose rates recorded corresponded to one or two pulses per 100 seconds. It was not possible to record lower dose rates by measuring for longer periods of time, as background counts in the ROI range from 1 to 10 counts per 100 seconds.

To compare dose rates at different energies, an estimate is made of the number of pulses in the region ignored because of the discriminator cut-off. This was carried out by assuming an exponential shape for the pulse height spectrum in the cut-off region. If a single radiation source was used, the dose rate was found to be proportional to the count rate (figure 4.15) but this was not the case if different radiation sources were employed. The average energy deposited per interaction was the same for radiation from a single source, but will obviously differ between different radiation sources (cf. figure 4.13). The absorbed dose is the energy deposited per unit mass of the radiated material ($1 \text{ Gy} = 1 \text{ J}\cdot\text{kg}^{-1}$), and a measure of the energy so deposited in the diamond must be used as an indication of the dose, not a measure of the number of interactions (i.e. counts).

The energy deposited by a γ -ray interaction corresponds to the size of the electric pulse it produces and should thus be proportional to the channel number. Thus the total energy deposited is proportional to the number of events per channel, $n(c)$, multiplied

by the channel number, c , and can be represented mathematically by

$$Dose = k \sum_{\text{all channels}} c \cdot n(c) \quad (4.1)$$

or

$$Dose\ rate = k \sum_{\text{all channels}} c \cdot r(c) \quad (4.2)$$

where $r(c)$ represents the count rate per channel, and k is a constant of proportionality which will depend on the pulse amplification and the radiation energy to pulse height conversion ratio of the particular diamond. The diamonds differ in response because of different concentrations of recombination and trapping centers, which reduce the number of charge carriers and thus the pulse height.

The diamond's dose rate response, described by equation 4.2, was calculated in units of k (i.e. using a value of $k = 1$) and was plotted as a function of the radiation dose rate (figure 4.17). The response between different sources corresponds far better than the response described by the count rate, but some discrepancy still exists.

It was thought that the silver epoxy and gold leads may scatter the radiation sufficiently to effect the response differently at different energies. The gold leads and silver loaded epoxy were removed and replaced with carbon fibre leads, attached to the diamond with a carbon epoxy dag. The ^{60}Co γ -ray response was reduced by approximately 25 %, indicating that the silver epoxy and gold leads are responsible for scattering of radiation and thus affect the pulse counting response. The response as a function of dose rate indicates a good correlation between the ^{60}Co and the ^{137}Cs γ -ray radiation sources (figure 4.18).

The pulse height spectra for the diamond with carbon fibre contacts was also exponential in shape, indicating that scattering by the contacts was not responsible for the pulse height distribution. An additional advantage of using carbon fibre contacts, is that the whole detector becomes tissue equivalent and thus will not disturb radiation fields during in-vivo measurements.

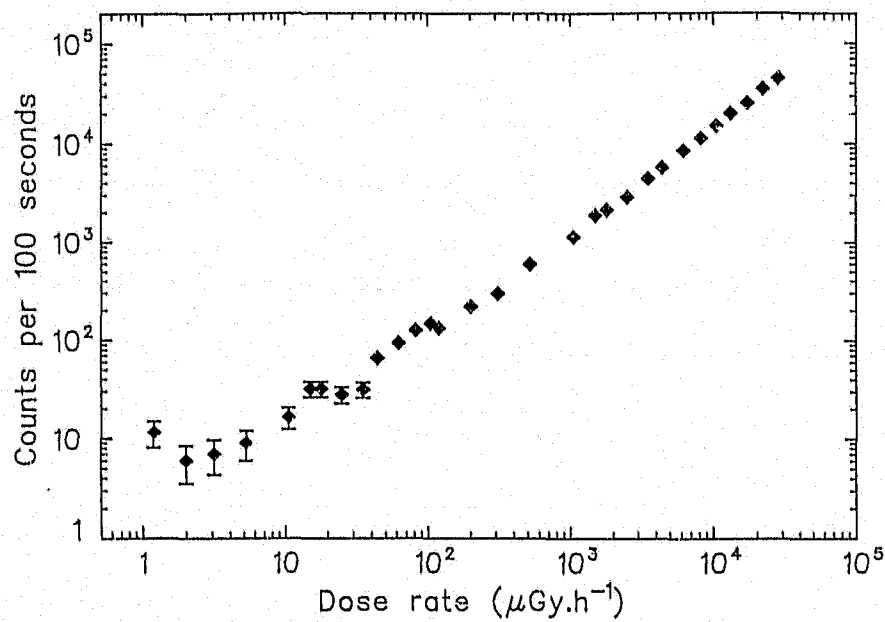


Figure 4.15. Count rate as a function of the dose rate of ^{137}Cs γ -rays. Diamond: Suite 2.

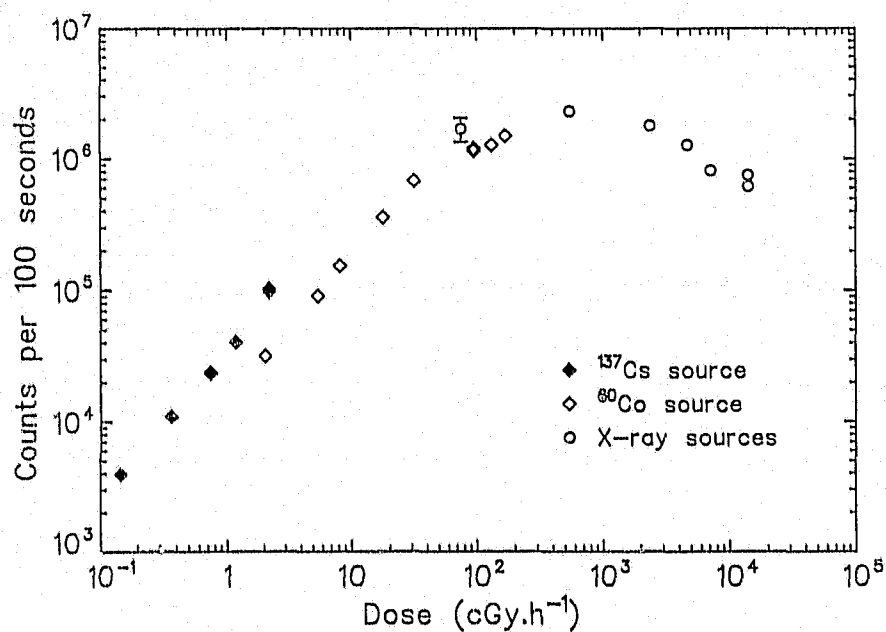


Figure 4.16. Count rate for irradiation from different sources. High count rate 'saturation' occurs because of electrical shorting (see text). Diamond: Suite 2.

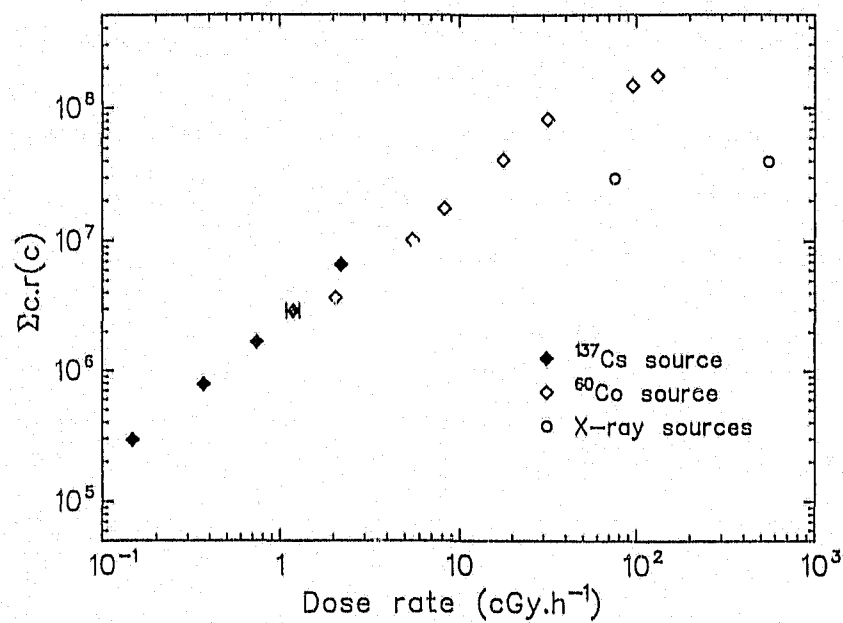


Figure 4.17. Dose rate response for irradiation from different sources. Gold leads attached to contact surface by means of silver loaded epoxy adhesive. Diamond: Suite 2.

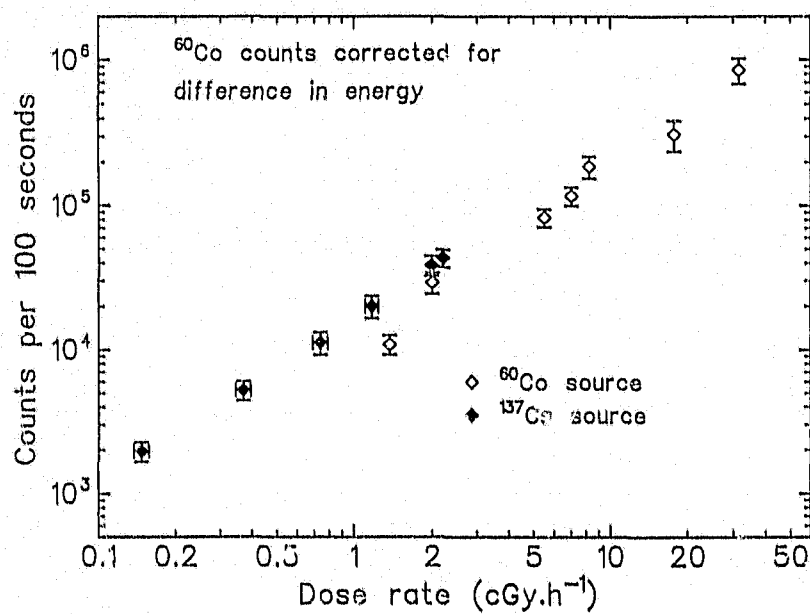


Figure 4.18. Dose rate response for diamond with carbon fibre contacts attached by means of carbon epoxy dag. Diamond: Suite 2.

The synthetic diamonds used have limitations in both the maximum and minimum dose rates that could be measured. The minimum dose rate was limited by the sensitivity of the pulse counting response and was in the region of 1 to 10 $\mu\text{Gy}\cdot\text{h}^{-1}$ (normal background levels are approximately 0.1 $\mu\text{Gy}\cdot\text{h}^{-1}$). At the minimum dose rates recorded, counted pulses and counts due to noise were approximately the same in number, it was thus not possible to measure lower dose rates by recording pulses for longer periods of time.

At dose rates greater than 1 $\text{Gy}\cdot\text{h}^{-1}$, large pulses (0.5 to 1 ms long as opposed to the radiation induced pulses of about 20 ns in length) were visible on the oscilloscope and are believed to be due to 'electrical shorting' between the diamond contacts. A radiation induced pulse occurring at the same time as a 'shorting' pulse was partially engulfed by the larger shorting pulse and was recorded as being smaller in size, thus resulting in a lower count rate. This process accounts for the apparent 'saturation' in the count rate at high dose rates (figure 4.16).

It is believed that ionization between metal inclusions occurring at high dose rates caused electrical current to flow along an ionized path through the diamond. The path remained partially ionized because of the large current flow, but was observed on the oscilloscope to decrease as a function of time and stop after about a millisecond. The dose rate at which 'shorting' was first observed was found to increase as the potential between the contacts was reduced.

A high nitrogen diamond (CoFe stone 6, 122 ppm nitrogen) was also used to measure dose rates. It was able to measure dose rates three times higher than those measured by the low nitrogen diamond (Suite 2, 7 ppm nitrogen) before the advent of shorting. It is believed that the improved maximum dose rate limit is the result of fewer impurities and metal inclusions in the high nitrogen diamond. It is interesting to note that the response from the high nitrogen diamond is approximately a third of that of the low nitrogen diamond. (cf. Chapter 7 for the nitrogen impurity in diamond). It is also believed that both the present maximum and minimum dose rate limits will be improved by using diamonds with lower impurity and defect concentrations.

Chapter 5. THE EFFECT OF LIGHT

5.1 Introduction

It is well known that diamonds absorb light, and that light affects the conduction properties of diamonds by filling and emptying of traps. Optical absorption, photoluminescence, photoconduction and recently thermoluminescence have become valuable tools in characterizing the trapping levels in diamonds. It is thus logical to assume that light will affect the pulse counting properties of diamonds.

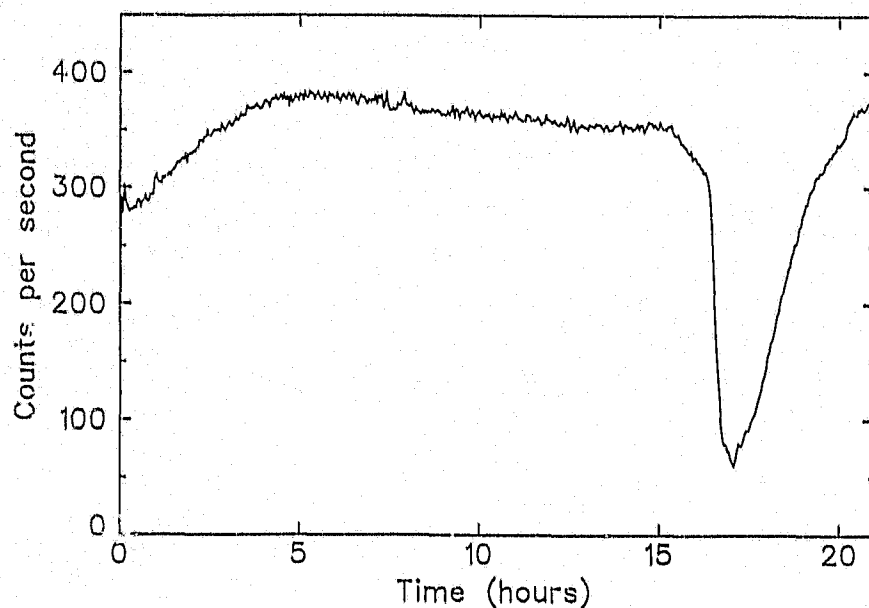


Figure 5.1. Diamond counting overnight in the dark. Drop in count rate after $16\frac{1}{2}$ hours corresponds to sunrise and sunlight incident directly on the diamond. Rise in count rate occurs after the sun has risen so that sunlight is no longer incident directly on the diamond. Diamond: Suite 2 (not yet implanted).

Initially the pulse counting measurements were performed with the diamond exposed to ambient light. It was soon realized that ambient light was affecting the pulse counting properties, and all subsequent measurements were carried out with the diamond in the dark. An interesting example of the affect of light occurred when the suite 2 diamond was left counting overnight in the dark (figure 5.1). The count rate increased initially as trapping levels were filled, then remained at a saturation value until a huge unexpected decrease occurred. Initially this decrease was unexplainable, but the time that the decrease occurred was found to correspond to sunrise. Sunlight shining on the diamond depopulated trapping levels and created a large background photocurrent, resulting in a decrease in the number pulses recorded. After the sun rose past a certain point, sunlight was no longer incident directly on the diamond, and the pulse counting rate recovered. Another example is shown by the thermoluminescent spectra in figure 5.2. The shallow thermoluminescent traps depopulate at room temperature (figure 5.2, Nam 1989). The time between irradiation and the thermoluminescent measurement was shorter for curve 'A', fewer shallow traps depopulated before the measurement and thus more counts occur in the region 20 - 70 °C, than for curve 'B'. Since the diamond in curve 'A' was exposed to ambient light the deeper traps depopulated and fewer counts occur than for curve 'B' at temperatures greater than 70 °C.

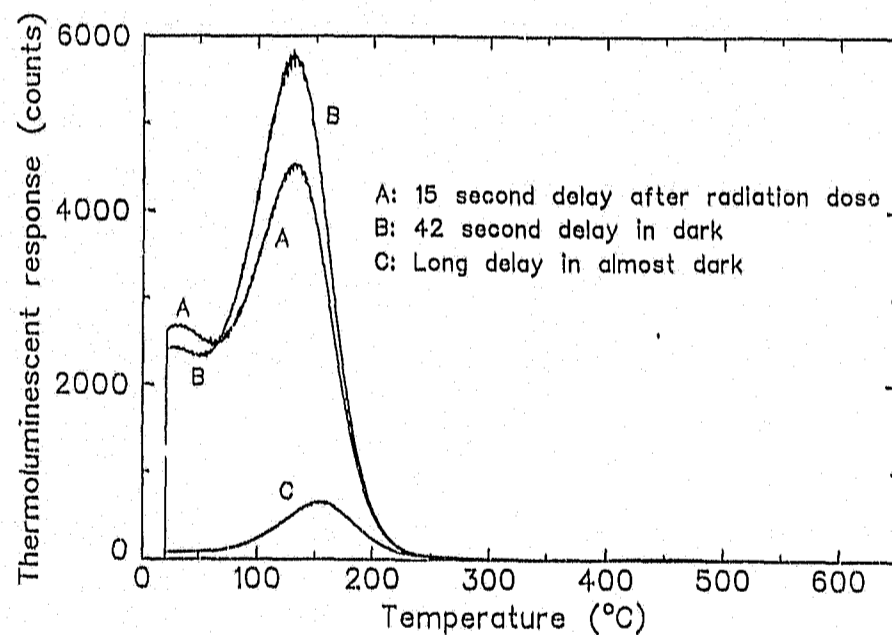


Figure 5.2. Thermoluminescent spectra of diamond suite 2 no. 2.

The major effect to be observed by pulse counting with the diamond not exposed to light, was the increase in response from diamonds with less than 60 ppm nitrogen concentration after being exposed to a large γ -ray dose (subsequent exposure to light returning the diamonds to the unprimed state, cf. section 4.4). The γ -ray pre-irradiation creates many charge carriers, filling the traps which would otherwise trap the charge carriers produced during pulse counting. Trapping of charge carriers reduces the size of the pulse to be counted, and thus results in fewer pulses in the ROI. The response of a diamond, not primed by pre-irradiation, increases slowly as traps are filled (figure 4.8), but the same diamond after pre-irradiation has a constant high count rate. When exposed to light the trapping levels depopulate, resulting in smaller pulses and a reduced count rate. This fact has been used to establish the energy of the trapping level.

Similar results have been observed in other investigations, Burgemeister (1982) reports that low nitrogen synthetic diamonds and a natural IIa diamond, used to measure d.c. conduction response to radiation, could be primed by irradiation to give a larger response, but if exposed to white light returned to the unprimed state. Keddy (1988) also measuring d.c. conduction response to radiation, reports that diamonds with single substitutional nitrogen concentrations of 1 – 10 ppm show a gradual increase in response while being irradiated, but diamonds with nitrogen concentrations of \approx 60 ppm exhibit a lower but more regular response. Willardson and Danielson (1950), Urlau et al (1961) using one type IIa and two type I diamonds, Vermeulen and Nabarro (1967b) using type Ia diamonds all report an increase in pulse counting when the diamond is exposed to red light and the latter two report a decrease with exposure to green light. In the above investigations the diamonds were exposed to the light during the pulse counting measurements, but for the measurements reported in this thesis, exposure to light and pulse counting were done separately so as to eliminate problems due to photocurrents during pulse counting.

5.2 Photoconduction

Photoconduction spectra of most of the diamonds were measured, to get an indication of trapping level energies. A Bausch & Lomb high intensity monochromator with a diffraction grating and a xenon light source was used to select monochromatic light in a range of 350 to 800 nm.

Author Fallon P J

Name of thesis Synthetic diamonds as Pluse Counting Radiation Detectors 1989

PUBLISHER:

University of the Witwatersrand, Johannesburg

©2013

LEGAL NOTICES:

Copyright Notice: All materials on the University of the Witwatersrand, Johannesburg Library website are protected by South African copyright law and may not be distributed, transmitted, displayed, or otherwise published in any format, without the prior written permission of the copyright owner.

Disclaimer and Terms of Use: Provided that you maintain all copyright and other notices contained therein, you may download material (one machine readable copy and one print copy per page) for your personal and/or educational non-commercial use only.

The University of the Witwatersrand, Johannesburg, is not responsible for any errors or omissions and excludes any and all liability for any errors in or omissions from the information on the Library website.